Norges miljø- og biovitenskapelige universitet

Master's Thesis 2016
30 credits

Norwegian University of Life Sciences
Faculty of Environmental Science and Technology
Department of Ecology and Natural Resource Management (INA)

Effects of low frequency acoustic pulses on startle behaviour and EOD activity in elephantnose fish (*Gnathonemus petersii*).

Hans Christian Sørnes Karlsen
Master / Lektorutdanning i realfag (LUR)

Acknowledgements

This master thesis was conducted at the Marine Biological Station Drøbak, University of Oslo (UiO), during spring 2016, as part of my master degree at Department of Ecology and Natural Resource Management (INA), Norwegian University of Life Sciences (NMBU).

The research project of my thesis was proposed by Associate professor Hans Erik Karlsen (UiO), and carried out in his lab at the Marine Biological Station under his supervision. My internal main supervisor for the thesis project was Professor Thrond Oddvar Haugen at INA. I would like to thank Hans Erik Karlsen for all his assistance in carrying out the exciting experiments, and for all his advice in the writing of the thesis. I would like to thank my main supervisor Thrond Oddvar Haugen at INA for all his help with statistics, conversations and valuable comments to the master thesis. My work was part of ongoing research at the Marine Biological Station into behavioural responses in fish, cephalopods and crustaceans to sound pulses. The aim of this work is to understand more about the mechanisms of how these different groups of pelagic animals respond to sound, and thus how they may be affected by increasing levels of anthropogenic sound and noise in the aquatic environment. I would like to thank co-workers at the Marine Biological Station, i.e. Post doc Maria Wilson, PhD student Rune Roland Hansen, research assistant Jens Ådne Rekkedal Haga and technical assistant Grete Sørnes, for all their invaluable assistance and fruitful comments and discussions of my thesis work. They all contributed in making my stay at the Marine Biological Station in Drøbak very interesting, educational and memorable.

Drøbak, August 2016

Hans Christian Sørnes Karlsen

Table of Contents

Abstract

Fast start and short-duration acoustic startle behaviour (C-response) are performed by fish, cephalopods, crustaceans and other animals in order to successfully evade abrupt threats such as attacks by predatory fish. In the present master thesis, the sensory system initiating C-response and electric organ discharge (EOD) response in the hearing specialist elephantnose fish was studied in an experimental swing chamber set-up. The swing chamber is specially designed for producing controlled low frequency acoustic stimulus waveforms. The waveforms studied in the experiments were single cycle sinusoids of initial acoustic pressure and particle acceleration in the frequency range 10 Hz to 30 Hz, and mimicked key components in the acoustic signature of charging predatory fish attacks. The aim of the study was to reveal how initial acoustic pressure and particle acceleration trigger the inner ear sensory system in elephantnose fish to produce acoustic EOD- and C-responses.

Acoustic startle behaviour was found to be optimally triggered by a combination of acoustic particle acceleration and compression, and very rarely by the same level of acoustic particle acceleration and rarefaction. Startle behaviours were highly directional, and this was ascribed to inner ear detection and coding of the direction of the initial particle acceleration. In the centre of the test chamber, acoustic startle behaviours were triggered by the particle acceleration component alone, but at significantly lower probability than when combined with compression. Startle behaviours observed in response to the low frequency stimuli greatly extended the known audible hearing range in elephantnose fish. Contrary to general opinion within the field of fish hearing, it was shown that acoustic pressure sensitivity is of behavioural relevance at very low sonic and infrasonic frequencies. The results of the study support the view that acute acoustic pressure sensitivity evolved independently several times in fish as adaptations to perform differentiated and more adaptable escapes from striking predatory attacks. EOD-responses were produced by the acoustic stimuli, and were significantly stronger to compression stimuli than to rarefaction stimuli. Why elephantnose fish emit a strong burst of EODs during acoustic startle behaviour is unclear, but may perhaps be as a distraction of electro-sensitive predators.

1 Introduction

Background

The aquatic environment is highly acoustic with numerous biological and non-biological sound sources. Important physical sources of low frequency sonic and infrasonic (< 20 Hz) sound in the ocean are turbulence due to ocean currents, seismic motions of the ocean floor, wind generated surface waves and ocean wave refractions at continental ridges and islands. Many such sources have fixed locations, and produce directional patterns of low frequency sound (an acoustic landscape) that may guide fish on migrations (Sand and Karlsen, 1986; 2000). Biological sound includes low frequency (< 50 Hz) water movement produced by swimming animals as well as charging predators (Kalmijn, 1989; Bleckman et al., 1991). In addition, many aquatic animals, including most fish, produce communication sounds by the grinding of specialized body parts, vibrations of gas-filled bladders and more. Frequencies of biological communication sounds in fish vary depending on hearing abilities, and typically range from about 50 Hz an up to about 500 Hz (see Fine and Parmentier, 2015).

It is well established that inner ear otolith organs in fish are highly sensitive to sound particle accelerations, and that this sense is of key importance for low frequency hearing in fish, and for successful startle behaviour evasion of charging predatory attacks (Sand and Karlsen, 1986; Karlsen, 1992a; 1992b; Karlsen et al., 2004). In the startle response, the prey fish detects the low frequency water acceleration present in the bow wave produced by the charging predator, and escapes (jumps away) in an appropriate direction. In addition to particle acceleration, many fish with elastic gas-filled bladders are indirectly sensitive so sound pressure. In these fish, sound pressure variations cause bladder vibrations which reach and stimulate the inner ear otolith organs. Acoustic pressure sensitivity is generally thought to be relevant for fish only at high frequencies (> 50 Hz). However, contrary to this wide spread opinion, it has been shown that low frequency sonic and infrasonic pressure may be of crucial importance in startle behaviour and predator avoidance is fish (Karlsen, et al., 2004; Eckroth, 2008; Hegvik, 2014). This discovery has relevance for the question of why acute acoustic pressure sensitivity has evolved independently several times in fish, i.e. in order to better avoid predation through startle behaviour or for high frequency acoustic communication. This has recently been referred to as "*one of the riddles of sensory*

physiology" (Ladich and Schulz-Mirbach, 2016). The present study has been aimed at shedding more light on this question by examining the effects of low frequency acoustic particle acceleration and pressure on acoustic startle behaviour in the species elephantnose fish (*Gnathonemus petersii*, Günther, 1862) family Mormyridae. The elephantnose fish belongs to a primitive order of teleost fish, and has a very unique specialization for high acoustic pressure sensitivity (Crawford, 1997).

Hydrodynamic signature of charging predatory fish attacks

Attacks by forwardly charging predatory fish are known to produce mainly low frequency (< 50 Hz) water movements and pressure waves (Bleckman et al., 1991). In front of the predator, a bow wave will be created consisting of initial particle acceleration directed away from the predator, and associated with an initial pressure increase (compression) (Eaton and Popper, 1995; Eaton et al., 1995). In the wake of a moving and charging fish, the hydrodynamic water movements will be opposite, and consist of water movement towards the fish associated with a pressure decrease. With respect to predator avoidance, the optimum response by the prey fish would be to perform an abrupt evasive startle response in the overall direction of the initial acceleration if the initial pressure phase is a compression. If the initial pressure phase is a rarefaction, the appropriate response should be against the initial acceleration or alternatively not to respond. In the carp fish hearing specialist roach (*Rutilus rutilus*), a differentiated acoustic startle behaviour was indeed found (Karlsen et al. 2004) by the fish executing a startle behaviour in response to a compression stimulus, and only rarely so to a rarefaction stimulus. The same startle behaviour pattern has later been shown to exist in the clupeid fish hearing specialist sprat (*Sprattus sprattus*) as well (Eckroth, 2008; Hegvik, 2014). Roach and sprat have very different adaptations and mechanisms for their acute acoustic pressure sensitivity, and they both differ from the acoustic pressure adaptations in elephantnose fish (see Figure 1.4). The question is whether elephantnose fish have the same ability to tune its startle behaviour according to pressure phase, or if they behave differently from other systematic groups of fish hearing specialists.

Weakly electric fish of the order Osteoglossiformes

Elephantnose fish are small, 7 cm – 12 cm long, weakly electric fish within the family Mormyridae in the fish order Osteoglossiformes (bony tongued fish) (Figure 1.1). The order

Figure 1.1 Elephantnose fish are small (7 cm – 12 cm) weakly electric fish found in freshwater river systems in West and Central Africa. They have a unique "nose", which is in fact a chin extension filled with electrosensory organs, and referred to as the *Schnauzenorgan*. Photo H. C. Sørnes Karlsen.

Osteoglossiformes includes approximately 245 living freshwater species within two suborders Osteoglossoidei and the Notopteroidei. It is considered a relatively primitive order of ray-finned fish which evolved in the Gondwane period before this continent broke up (Hopkins, 1986). Today, Osteoglossiformes are found in South America, Africa, Australia and southern Asia.

The Mormyridae family is located to freshwater river systems in West and Central Africa. It is the most diverse group of weakly electric fishes within the Osteoglossiformes, with more than 200 different species (Hopkins, 1986). Elephantnose fish, in particular, is a nocturnal species which mainly live on small planktonic organisms such as mosquito larvae and small crustaceans. They have several highly specialized and derived sensory adaptations in order to survive and thrive in a dark, turbid and often hostile aquatic environment. Their light sensitivity is extraordinary high by an adaptation of elongated rods and cones grouped together as "macro-receptor" units into round retinal cups ensheathed by reflecting guanine crystals (Kreysing et al., 2014). Light sensitivity is increased by a factor of up to 50 by photons being reflected and focused on the photoreceptive cells in the crystal cups (see Lansberger et al., 2008; Kreysing et al., 2014; Liu et al., 2016).

Electroreceptors and electric organ discharges in elephantnose fish

Elephantnose fish have a highly specialized ability for passive electro-detection and location of objects, active electrolocation and of electrocommunication. In their tail region,

elephantnose fish have modified muscle cells called electrocytes which emit very short duration (≈ 400 μs) and weak (up to 5 V) electric pulses called electric organ discharges or EODs. The discharge frequency varies between 1 Hz and 100 Hz, and depends on the behavioural context. The electric field produced surrounds the fish (Figure 1.2), and is continuously detected and analyzed by highly sensitive electroreceptors (ampullary organs, mormyromasts and knollenorganen) in the skin of the fish. Any distortions of the field by external objects are immediately detected by the fish, giving the fish an active electrolocation sense reaching out a distance of about one body length. In the so called "nose" of the fish, which is a chin extension and not a nose, there are numerous electro-sensitive organs, and the "nose" (Schnauzenorgan) functions as a fovea of the electric sense in the fish (Engelmann et al., 2009).

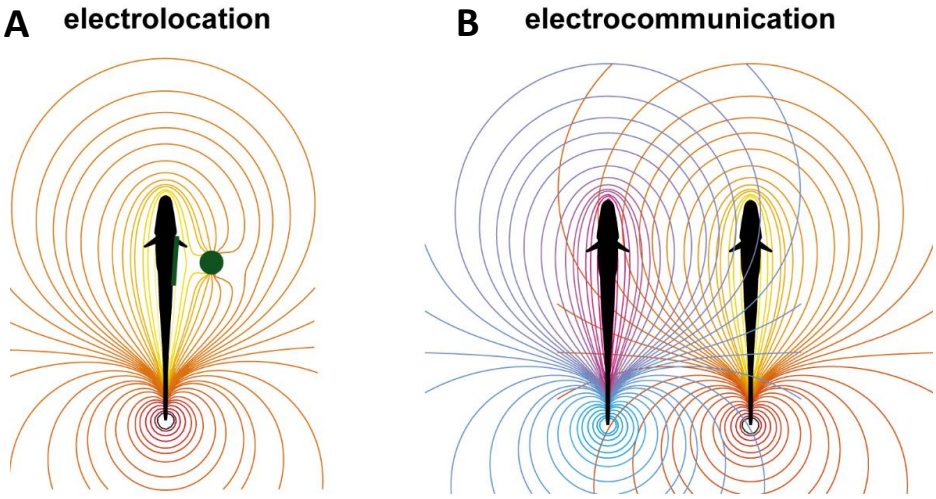

Figure 1.2. (A) The electric organ in the tail of elephantnose fish emits EODs at a variable rate of 1 Hz to 100 Hz. The field and any distortions of it by external objects are continuously monitored by electroreceptors (mormyromasts) in the fish skin. (B) One way of communication in elephantnose fish is by detection of electric fields from neighbouring fish by especially dedicated electroreceptors (knollenorganen). Pictures obtained by permission from Electric fish www blog, 2016.

A well-known EOD-response linked to electro-perception in weakly electric mormyrid fish species, is a sudden and transient increase in the EOD-rate (shortening of inter-EOD intervals) when a nearby object is suddenly altered in its properties. This so-called "novelty response" can be regarded as an active electrical orientation mechanism due to new sensory input (Engelmann et al., 2009). The EOD-response or awareness response can be evoked by electrical, acoustical, visual and mechanosensory lateral line stimuli as well as multi-model

stimuli. In the present study, the EODs were continuously recorded and EOD-responses were measured to the acoustic stimuli employed.

Sound detection in elephantnose fish and other fish hearing specialists

In addition to their specialized visual and electric sense, mormyrid fish like the elephantnose fish are highly sound productive (300 Hz – 500 Hz), and have specialized adaptations for acute acoustic sound pressure sensitivity, i.e. they are fish hearing specialists (McCormick and Popper, 1984; Crawford, 1997; Fletcher and Crawford, 2001). Adaptations for sound pressure sensitivity have evolved independently several times in teleost fish (see Figure 1.4). Today more than 32% of all living fish species are fish hearing specialists, and acoustic pressure sensing must, thus, have had a strong adaptive value. The mechanisms of hearing in fish are currently well understood (see Popper et al., 2003). Briefly, the inner ear contains three pairs of otolith organs which each function as equilibrium organs, as gravity detectors and as hearing organs. A sketch of an otolith organ is shown in Figure 1.3. Each organ is in essence a fluid-filled vesicle with a dense otolith (ear stone) mechanically coupled to displacement and directional sensitive hair cells. When a fish is accelerated in a sound field, the otolith will lag behind the movements of the rest of the fish, including the hair

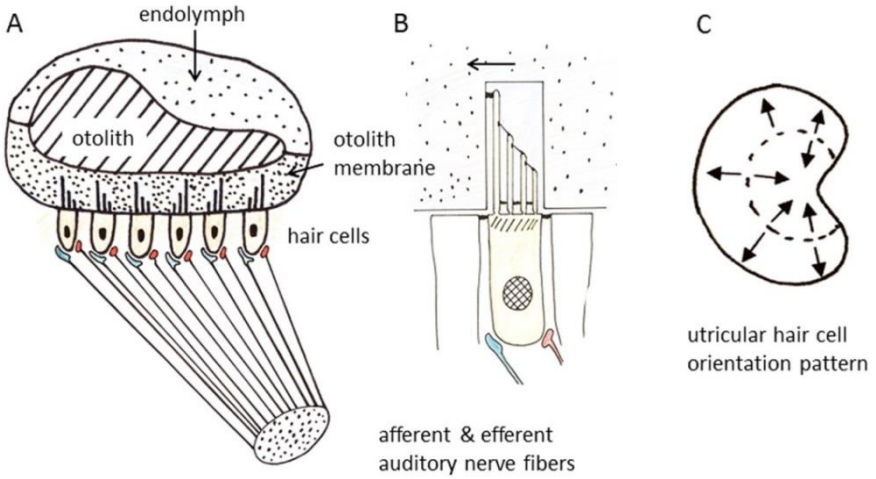

Figure 1.3. (A) Fish otolith organ (cross section). Each otolith organ is in essence a fluid filled vesicle containing a calcium carbonate otolith overlaying an epithelium of sensory hair cells. **(B)** The stiff apical hair bundle of the hair cells is mechanically coupled to the otolith via a gelatinous otolith membrane. A thin water film separates the hair cells and otolith membrane. Hair cells are only stimulated by hair bundle deflections in the direction (arrow) of the tallest sensory hair (the kinocilium). **(C)** The arrows show the direction of hair cell orientations and sensitivities in the otolith organ. Different hair cell orientations make the otolith organ sensitive to overall fish acceleration in different directions. Modified from sketch by H. E. Karlsen.

cells, because of it's larger inertia. This causes relative movement between the otolith and the hair cells, and thereby stimulation of the hair cells. In this way all fish are directly sensitive to the acoustic particle acceleration. Hair cells in an otolith organ have different axis of maximum sensitivity. Therefore, otolith organs are directional sensitive organs making it possible for the fish to determine the directionality of an acoustic stimulus.

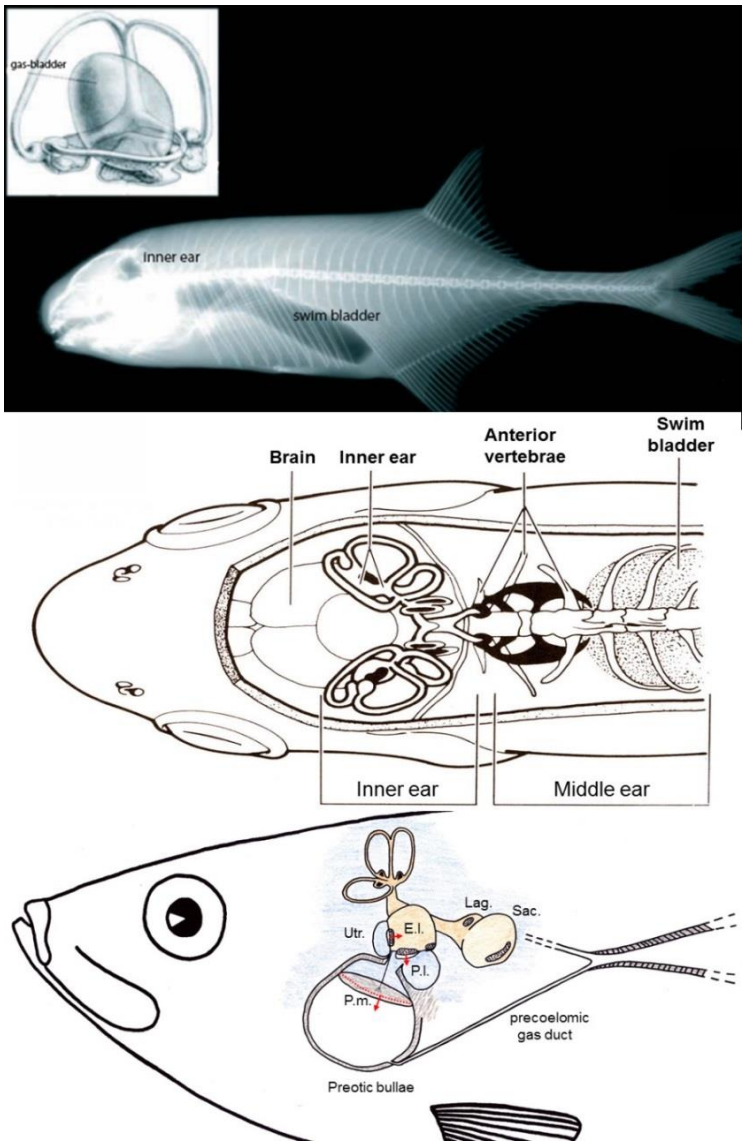

Figure 1.4. Illustrations of three highly different specialized adaptations for acute acoustic pressure sensitivity in fish. In weakly electric fish (Osteoglossiformes) (top) acoustic pressure variations are effectively transferred to the inner ear via a small gas vesicle derived from the swimbladder and closely associated with the saccule otolith. In carp fish (Cypriniformes) and catfish (Siluriformes), sound pressure induced swimbladder vibrations are transferred to the inner ear saccule otolith by a specialised chain of ossicles (shown in black). In clupeid fish (Clupeiformes) (bottom), forward extensions of the swimbladder end in a gas-filled vesicle closely associated with the inner ear utricle otolith. Illustrations top down from Fine and Parmetier (2015), Popper et al. (2003) and Karlsen and Eckroth (2011).

Sensitivity to sound pressure in fish is always associated with gas-filled elastically structures, i.e. the swimbladder or gas-filled structures derived from the swimbladder. Gas is much more compressible than water, and sound pressure induced volume pulsations of the gas-filled structures may constitute a significant mechanical stimulation of the inner ear. In fish hearing specialists, specialized mechanisms for effective transfer of such mechanical energy to the inner otolith organs has evolved. Three examples of such adaptations are shown in Figure 1.4. It is still unresolved and a quite puzzling question why such adaptations have evolved independently several times in teleost fish. Possibly, it is related to predator-prey relations, and the evolution of fast start and short duration evasive startle behaviour in fish. If this is the case, the fish must be sensitive to very low frequency (< 50 Hz) acoustic pressure. This has been shown for Cypriniformes and Clupeiformes. In Osteoglossiformes, hearing sensitivity has so far only been studied in elephantnose fish and only in the frequency range 100 Hz – 2500 Hz (McCormick and Popper, 1984; Fletcher and Crawford, 2001). Thus, it is still an open question whether fish hearing specialists in this order are able to detect acoustic particle accelerations and pressures in the low frequency sonic and infrasonic range.

Acoustic startle behaviours in fish

Fish have an extraordinary ability to perform fast-start and short-duration escape behaviours (startle responses) in order to evade life threatening situations (see Eaton et al., 2001). Even though startle responses may be triggered by vision and lateral line stimulation, the main stimulus for eliciting this behaviour in fish appears to be acoustic stimuli activating the inner ear (see Eaton et al., 2001). Pressure is a scalar quantity and without directionality. A startle behaviour directed away from the threatening stimulus must therefore rely on directional information from the inner ear, the skin lateral line system and/or the visual system.

In nature, startle responses are initiated when either of two huge spinal neurons, called Mauthner cells, are activated (see Faber et al., 1989; 1991; Korn and Faber, 1996; Zottoli and Faber, 2000; Eaton et al., 2001). Mauthner cells receive direct sensory information from the inner ear, the skin lateral line system, the visual system and skin mechanosensory nerves (Figure 1.5). They connect directly to spinal motor neurons innervating most contra- and ipsilateral body muscles. When one of the Mauthner-cells

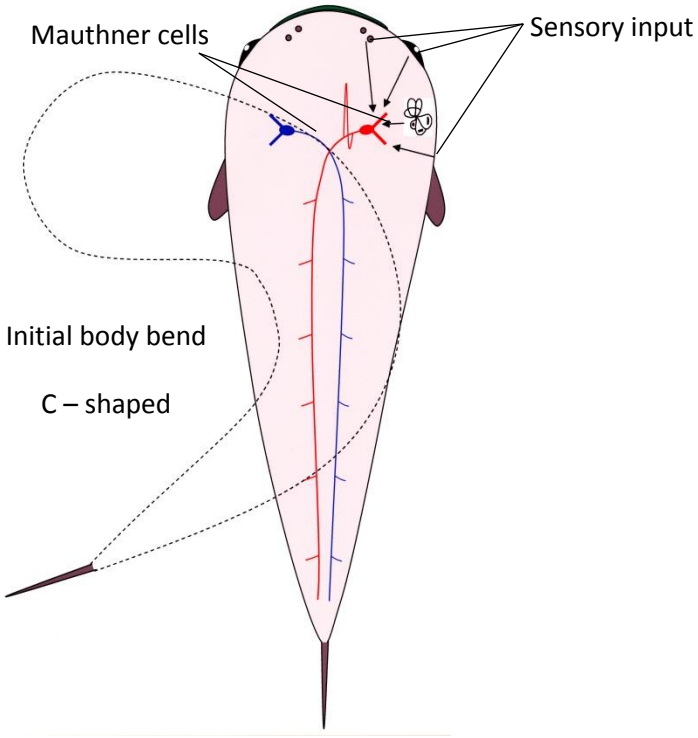

Figure 1.5. Sketch illustrating parts of the brainstem escape network (BEN). Two Mauthner cells (coloured as red and blue in the sketch) integrate neural input from ipsilateral sensory organs (olfactory, eye, inner ear, lateral line system and skin receptors). When Mauthner cells are activated, contra lateral body musculature is stimulated and the fish body forms the defining initial body C-bend of the startle response. The still unanswered question is how the Mauthner-cells and the rest of the super-fast BEN system within a few milliseconds determines the correct initial C-bend away from threatening stimuli. Sketch by H. E. Karlsen.

reaches threshold, it fires a single action potential which triggers a contraction of contralateral trunk musculature, and at the same time an inhibition of ipsilateral body musculature. This causes a startle response defining initial C-bend of the fish body.

How acoustic pressure and acceleration triggers and determines the directionality of startle behaviour (C-response) in different groups of fish is still unclear (Eaton et al., 2001; Karlsen and Eckroth, 2011). In this master thesis, the sensory and neurophysiological basis for startle responses in elephantnose fish were examined. An experimental swing chamber was used in which the test fish was subjected to an acceleration associated with an initial compression in one half of the chamber, and the same acceleration associated with an initial rarefaction in the other half of the chamber. Low stimulus frequencies of 10 Hz – 30 Hz were chosen in order to create acoustic stimuli which mimicked essential components of the hydrodynamic signal of predator attacks. EODs were continuously measured in the test fish

during acoustic stimulations since a change in EOD-rate, i.e. a novelty response, would show that the fish were able to detect the low frequency sound pulses. A key question in the study was whether elephantnose fish would perform typical startle behaviours in response to the test signals. In order to document this, high speed video recordings of fish behaviour was performed during testing.

Research hypotheses

H01: The hearing range of the weakly electric species elephantnose fish does not extend below the lower cut off frequency of 100 Hz determined in earlier studies.

Given that H01 is rejected, the following hypotheses will be examined:

H02: Behaviour responses in elephantnose fish to low frequency (10 Hz, 20 Hz and 30 Hz) acoustic waves are triggered and driven by acoustic particle motion and not by acoustic pressure.

H03: EOD-rate in elephantnose fish is not affected by low frequency (10 Hz, 20 Hz and 30 Hz) acoustic pulses.

H04: Sound pulses (10 Hz, 20 Hz and 30 Hz) induced evasive behaviours in elephantnose fish are not influenced by pressure phase, i.e. initial compression or initial rarefaction.

2 Materials and methods

Elephantnose fish acquisition and storage

Elephantnose fish were obtained from Oslo Dyrebutikk AS (Oslo) in June 2015. They were caught wild from the Niger River in Nigeria, and imported by Imazo AB (Vara, Sweden). At the Marine Biological Station in Drøbak they were kept, 6 animals each, in an enriched environment in three 300 l freshwater storage tanks (Figure 2.1). Elephantnose fish is sensitive to freshwater conditions (Fishlore, 2016). Therefore, the freshwater in the storage tanks was continuously filtered and regularly shifted. Freshwater was prepared from charcoal filtered tap water. This was aerated, and the following ion concentrations added to achieve a defined freshwater; 0.5 mM NaCl, 0.2 mM $CaCl_2$ and 0.05 mM KCl. The temperature of the water in the storage tanks and in the test chamber was 26°C. Test fish had been kept in the storage tanks for 6 months before testing began.

Figure 2.1. Elephantnose fish were kept in an enriched environment (freshwater plants and a variety of objects and hideouts) in 300 l storage tanks as shown in the photo. The Glava insulation was added to help keep the water temperature at 26°C. The door leads to the room with the experimental swing system set-up. Photo by H.C. Sørnes Karlsen.

Every morning and evening the elephantnose fish were fed chironomid larvae (Fina fisken, Tropehagen zoo, Vinterbro). Surplus food waste, not removed by filtering, was removed by a special made suction hose every morning prior to feeding. Water depth was continuously kept at ca. 30 cm in the storage tanks, the same depth and pressure was employed in the experimental set-up. The air temperature in the storage tanks room was

held at 22°C. Glava was used to insulate the storage tanks, and styrofoam plates were placed over the tanks to prevent water temperature loss. Elephantnose fish are very timid and nocturnal. The tanks need multiple hiding places in the form of plants, net tubes, pots and pipes, otherwise the elephantnose fishes will be stressed (Fishlore, 2016). Therefore, plants, small net tubes and small woods were used to make hiding places for the elephantnose fish in the storage tanks. A total of 9 elephantnose fish were studied in the experiments, which were conducted in accordance with the Norwegian Animal Act of 1974, the Regulation on Animal Experimentation of 1996 and approved by the Norwegian animal research authority (FOTS permission 15/205458-1).

Experimental swing set-up

Elephantnose fish were studied in an experimental swing set-up (Figure 2.2.) designed to create controlled low frequency acoustic acceleration and pressure stimuli. The set-up has previously been described (Karlsen, 1992a; 1992b, Karlsen et al., 2004; Eckroth, 2008; Hegvik, 2014). Briefly, the test chamber was a thick walled (3 cm) Perspex chamber (inner dimensions of 55 x 27 x 14 cm) suspended in four steel wires attached to a solid steel frame (Figure 2.2). The frame was mounted on a 150 kg concrete block resting on a 12 cm thick base of dry sand poured directly on a concrete floor on solid bedrock. The test chamber was sealed with a transparent Perspex lid and looking screws, and filled in such a way that no air bubbles formed within the chamber. A small flow of water circulated the chamber during the experiments. The water-filled test chamber and experimental animals were accelerated by driving voltage waveforms fed to two electromechanical vibrators (V20, DataPhysics Corp., Sane Jose, CA, USA) firmly secured to the concrete base of the set-up, and attached to each end wall of the test chamber via steel rods. The waveform to one of the vibrators was inverted allowing the vibrators to work in a push and pull mode. To avoid the possibility of elephantnose fish detection of any magnetic field, a Faraday cage covered the vibrators, electric cabling and the test chamber except for the transparent top plate. Voltage waveforms were generated by Spike software version 8.02 (Cambridge Electronic Design Ltd, Cambridge, UK) and a 500 kHz and 16 bit D/A- A/D converter (Micro 1401 mkII, Cambridge Electronic Design Ltd, Cambridge, UK). Before reaching the vibrators, the driving voltage waveform passed an attenuator (LAT-45, Leader Electronics Corp., Japan) for stimulus level adjustments and finally a custom build DC-power amplifier (40 W) set to fixed gain. To avoid

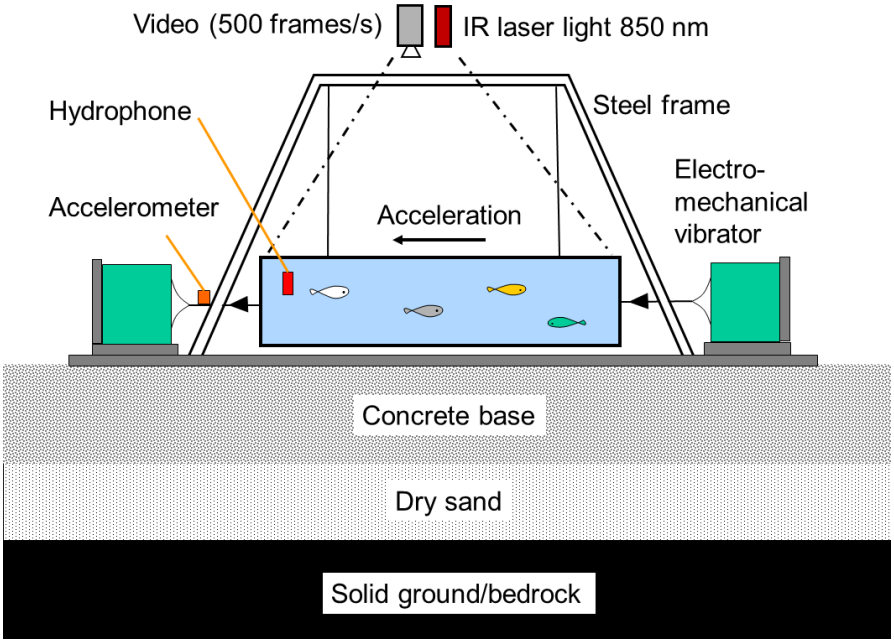

Figure 2.2. The experimental swing system consists of a water filled Perspex chamber suspended by four steel strings from a solid steel frame and driven by two electromagnetic vibrators. The horizontal movements of the swing chamber were continuously measured with an accelerometer. Pressures created inside the chamber were measured with hydrophones only during system calibration. The behaviour of the experimental fish inside the test chamber was monitored by high speed video recording (500 fps). EODs by the fish were recorded by 3 silver chloride wires entering 2 mm inside the chamber through the centre of the top plate (not shown in the illustration). Faraday cages were covered the electromechanical vibrators, electric wiring and the test chamber except for the top plate (not shown in the illustration). Modified from an unpublished sketch by H. E. Karlsen.

any disturbance of the animals during the experiments, the test chamber was located in a separate, dedicated room, remotely operated from a control room (Figure 2.3). The animals were continuously monitored on a computer screen by the high speed video camera (further described in a later section). Acceleration of the test chamber was continuously measured by high sensitive (4.0 ms^{-2} per V) accelerometer (Entran EGCS-A2-2, Les Clayes-sous-Bois, France) attached to the test chamber.

The different background accelerations of the experimental apparatus have previously been measured in 1/3 octave bands using a Brüel and Kjaer vibration meter type 2511 (Karlsen, 1992a; 1992b). In the frequency range 0.3 Hz – 1 kHz they were found to be below 10^{-6} ms^{-2}, or more than 30 dB below known infrasonic auditory acceleration thresholds of approximately 5 x 10^{-5} ms^{-2} in fish (see Sand and Karlsen, 2000). The background pressure variations in the swing chamber were below 60 dB re 1 µPa, measured in the centre of the

chamber in 1/3 octave bands in the frequency range 10 Hz - 200 Hz. Background noise levels were thus below the stimulus levels employed in the thesis, and most likely did not mask behaviour responses.

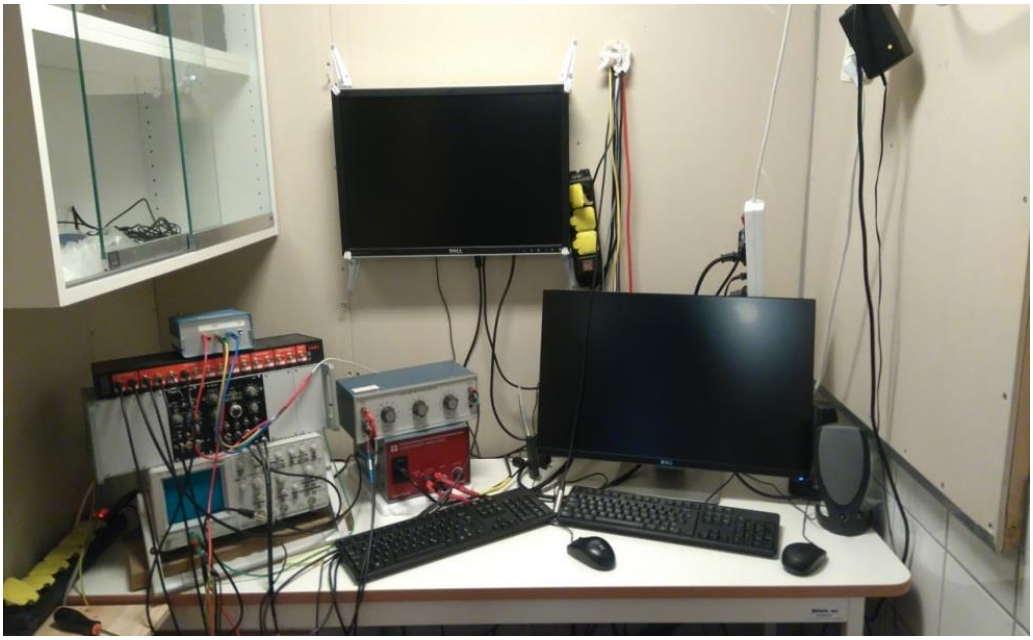

Figure 2.3. The control room for the experiments was separate from the experimental room containing the fish test chamber. The driving voltage waveforms to the vibrators were designed in the software Spike 2 version 8.02, and delivered by analogue to digital converters. The waveforms were level regulated in decibel steps by an attenuator, and subsequently amplified by a specially built 40 Watt DC (direct current) power amplifier. The power amplifier was set at full gain during the experiments in order to eliminate any electric switch on-off of transients. Separate computers controlled the high speed video recordings and the stimulus waveforms. Photo by H. C. Sørnes Karlsen.

Stimulus waveforms and system calibration

The stimulus waveforms in the current study were the same as those in earlier studies in the same set-up (Karlsen et al., 2004, Eckroth, 2008; Hegvik, 2014). Briefly, the voltage driving waveform to the electromechanical vibrators was a single cycle sinusoid voltage of frequency 10 Hz, 20 Hz or 30 Hz, which was DC shifted one peak amplitude and phase shifted -90° to start at zero voltage (Figure 2.4). The shape of driving voltage was chosen in order to avoid any on-transients in the initial displacement, velocity and acceleration of the test chamber. The driving voltage waveforms each caused a close to single frequency sinusoidal initial acceleration of the test chamber as well as a sinusoidal

initial pressure change in the leading and lagging halves of the test chamber (Figure 2.4). The acceleration of the test chamber was monitored in every experiment. However, since pressure calibration had recently been carried out in detail (Hegvik, 2014), this was not measured in this study. The stimulus acceleration levels were measured in the Spike software as 0-peak amplitude values in mV, and subsequently recalculated to ms^{-2} for the acceleration based on calibration of the recording devices given by the manufacturer. The corresponding pressure amplitudes at different locations in the test chamber were available from the study of Hegvik (2014). In the present study, stimulus levels are presented as amplitude rms (root mean square) values calculated as amplitude 0-peak values/$\sqrt{2}$). In the

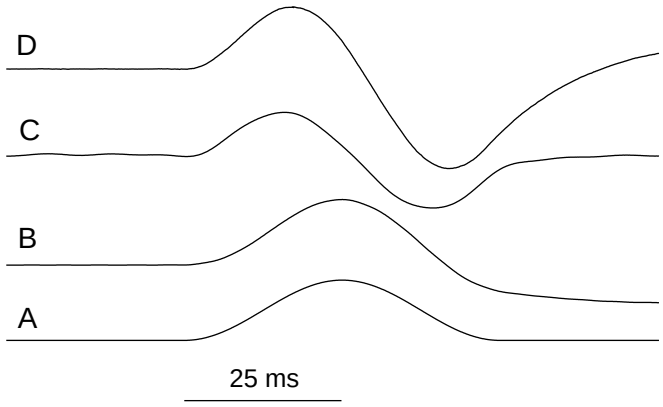

Figure 2.4. Illustration of the shapes of the driving voltage waveform and stimulus waveforms employed in the study (from Hegvik, 2014). The illustration is for the 20 Hz stimulus, but is representative also for the 10 Hz and the 30 Hz stimuli employed. **(A)** For all experiments performed, the driving voltage waveform to the vibrator was a single cycle sinusoidal voltage which was DC shifted one peak value and phase shifted to start at -90°. **(B)** Pressure waveform created 5 cm from the end wall in the lagging half of the swing chamber with a Reson hydrophone, i.e. without distortions from pre-amplification and filtering. The waveform closely approximated a 20 Hz single cycle sinusoid. The pressure waveform in the leading half of the swing chamber was identical in level but inverted 180°. **(C)** Acceleration of the test chamber measured by a high sensitive accelerometer. The initial acceleration of the swing chamber closely approximated a 20 Hz single frequency sinusoidal waveform. **(D)** Pressure waveforms recorded by a highly sensitive Sensor hydrophone. The waveform was slightly distorted due to low pass filtering and pre-amplification of the signal within the hydrophone head stage.

present study the frequencies 10 Hz, 20 Hz and 30 Hz were examined. Three stimulus levels of 0.04 ms^{-2}, 0.13 ms^{-2} and 0.4 ms^{-2} were employed for each stimulus frequency. The corresponding pressure levels in the rarefaction and compression AOIs (Figure 2.5) were 2.7 Pa (129 dB re 1 µPa), 8.8 Pa (139 dB re 1 µPa), and 27.2 Pa (149 dB re 1 µPa), respectively.

When the test chamber is accelerated by the driving voltage waveform, an initial acceleration associated with an initial pressure increase (compression) develops in the trailing half of the test chamber, while an acceleration associated with a pressure decrease is created in the leading half of the test chamber (Figure 2.6). Ongoing mathematical modelling of particle accelerations and pressures generated inside the test chamber (Karlsen, *personal communication, July, 2016*) have shown that at any instance of time following stimulus onset, there is a linear gradient of pressure inside the test chamber. Thus, in the centre of the test chamber there will be initial acceleration associated with no initial pressure change. A water movement inside the chamber and relative to the chamber walls is necessary to support the pressure differences created in the two chamber halves. It can be shown that maximum relative water movement will be in the chamber centre, and that it will be zero at the end walls. However, based on modelling of the set-up, it can be shown that the level of relative water movement was below 10^{-7} ms^{-2} for the maximum stimulus level of 0.4 ms^{-2} employed in the study. Particle accelerations associated with elastic compression and rarefaction of the water to create the pressure variations in the chamber were, in addition, far below the overall accelerations of the test chamber. This means that during stimulations, the same level of particle acceleration was experienced by the fish inside the test chamber irrespective of its position in the chamber. Still, in order to avoid any possible boundary layer effects, the fish were only tested when they were inside an AOI in the rarefaction and the compression halves of the chamber, respectively (Figure 2.5). The AOIs secured that the fish was at least about one body length from any side walls. Startle behaviour by the elephantnose fish in the centre of the test chamber was originally not a part of the planned thesis work. However, results from a few fish and stimulations at this position have been included in the study. The initial particle acceleration and pressure created in the trailing and leading half of the test chamber mimicked key hydrodynamic signatures of the front and wake of a charging predatory fish (Figure 2.6). The experimental set-up was therefore well suited to examine aspects of acoustic startle behaviours in fish.

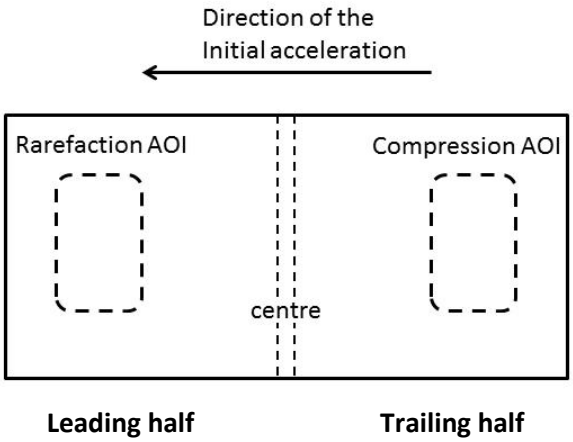

Figure 2.5. Top view of the experimental test chamber. When the chamber is accelerated, a compression develops in the trailing half, while a rarefaction is created in the leading half. In the centre there will be no initial pressure change. The acceleration experienced by the test fish was essentially the same at every location inside the test chamber. Test fish were stimulated when inside an area of interest (AOI) indicated by broken lines. The AOI was at a distance of 4 cm from the nearest side walls.

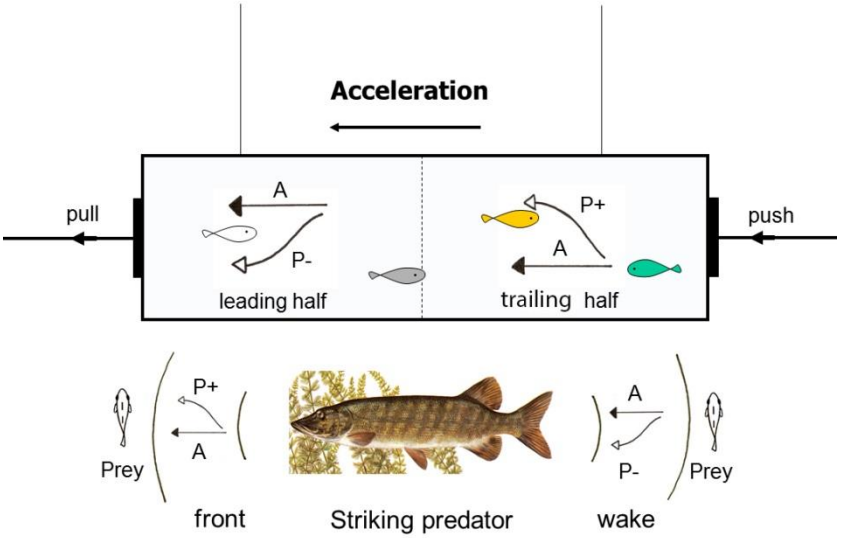

Figure 2.6. A cross sectional view of the test chamber. The initial particle acceleration and pressures created inside the rarefaction and compression AOIs in the test chamber mimics key aspects of the hydrodynamic signals created in the front and in the wake of a striking predator. The set-up is therefore suited to study how fish may respond behaviourally to such stimulus situations. Modified from a sketch by H. E. Karlsen.

Experimental procedures

A single test fish at the time was allowed to freely swim into a glass container placed in the holding tank, and then gently transferred to and allowed to swim into the experimental test chamber. This was all performed in very dim light conditions in order not

to stress the fish. The additional preparation of the test chamber by securing the lid by locking screws, removing any air bubbles and connecting the electromechanical vibrators took less than 3 minutes. After this all light was turned off, and the test fish allowed acclimatizing to the new surroundings for a period of 2-3 hours. During this period the EOD-rate declined and reached what was considered to be a relatively steady basal state. The test fish was subjected to two stimulations each of the 9 different stimuli employed with respect to frequency and level. Each of the 18 tests was assigned an integer number in the range 1 to 18, and testing was subsequently carried out according to a randomized sequence of these test numbers. In some individuals more testing was carried out. The time between tests varied between 10 - 25 minutes.

Measurements of electric organ discharges

EODs by the experimental fish were measured by three teflon coated silver wires (diameter 1 mm) which entered the chamber through the top lid. The tips of the silver wires were unshielded, chlorinated and placed just inside (2 mm) the test chamber. They were placed 4 cm apart, and this arrangement allowed for measurements of EOD-signals irrespective of the fish's position inside the chamber. The recording electrodes were fed to a differential pre-amplifier type BG48GX (NPI, Electronic Instruments, GmbH, Bauhofring, Germany), and recorded by the Spike 8.02 software (Cambridge Electronic Design, Cambridge, UK). In the Spike software each individual EOD was recognized and transformed into a 4 V event pulse. The software simultaneously stored the time of each EOD as well as time between EODs. This made it possible to measure pre-stimulus EOD-rates as well as EOD-rates following stimulus onset. EOD-pulses were very fast, and had duration of 300 µs to 400 µs. Their amplitude varied, and following an agitation of the animal the EOD-rate increased and often the amplitude of the EODs became slightly higher. The sampling rate of the analog to digital converter (ADC) was 20 kHz for the EOD-recordings. An example of an EOD-recording and a "novelty response" of increased EOD-rate is shown in Figure (2.7).

Video recording and startle response tracking and analysis

Experiments were conducted and videos of behaviour responses recorded in an infrared (IR) light setting using a sharply defined 850 nm laser light. Except for the laser light, the experimental room was totally sealed for any stray light. The elephantnose fish is not

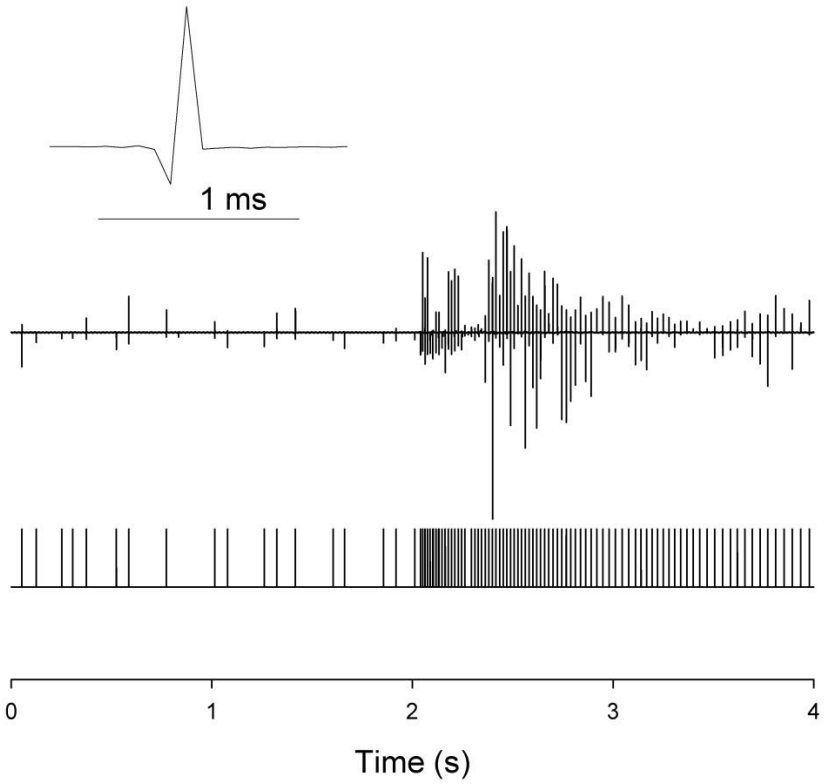

Figure 2.7. Example of a typical recording of EODs from an elephantnose fish in the test chamber (middle trace). The ADC sampling rate was 20 kHz. The lower trace shows the event pulse channel generated by the Spike v8.02 software as it identified each of the EODs, irrespective of their size. The software stored the time of the event and time differences between events. The inset (top left) shows a high magnification of an EOD sampled at 50 kHz. The duration of the recorded EOD was about 300 µs.

considered to be sensitive to near IR light in the 850 nm range (professor Gerhard von der Emde, *personal communication, July, 2016*), and the experiments were therefore considered to be performed in total darkness for the animal. IR video of the fish behaviours were recorded at 500 frames per second (fps) by an AOS S-PRI plus high speed film camera (HT-Holding AG, Switzerland). Individual video frames were stored as BMP format images, and imported to the video analysis program ImageJ (National Institute of Mental Health, USA). MTrackJ is an ImageJ plugin which facilitate frame by frame tracking of moving objects in image sequences, and this plugin was used to track movements of fish during startle behaviours and to measure startle response latencies. Synchronization of the spike driving voltage waveform and the high speed video recording was done by letting the Spike software generate an 8 V square pulse at stimulus onset, and feeding this pulse to a red LED bulb positioned above the test chamber and in the periphery of the camera view. The LED was on within 1 ms, and the first frame with the LED light on in this way showed the time of

stimulus onset. The LED light was positioned at the bottom of a 6 cm deep black cylinder and totally invisible to the test fish.

A fixed routine for the manual tracking (mouse positioning and clicks) of startle responses in MTrackJ was adopted. First, the four corners of the test chamber were traced (i.e. x, y coordinates determined and stored), and a distance calibration line added for conversion from pixels to mm. This was performed in the first frame of stimulus onset. The video was then stepped forward frame by frame until the first frame with a visible body movement (i.e. start of the startle behaviour). The position of the tail, the thorax and the head of the fish was then traced in the last frame before onset of body movement and the startle behaviour. This gave the initial position and orientation of the fish. The movement of the fish during the startle behaviour was then tracked by tracing the position of the fish's head in the last frame before onset of body movement and for the next 140 ms. Frame steps were set to 4 ms for this tracking. Startle movement, speed and distance were in this way recorded with 4 ms resolution for total startle duration of 140 ms. Coordinates were then

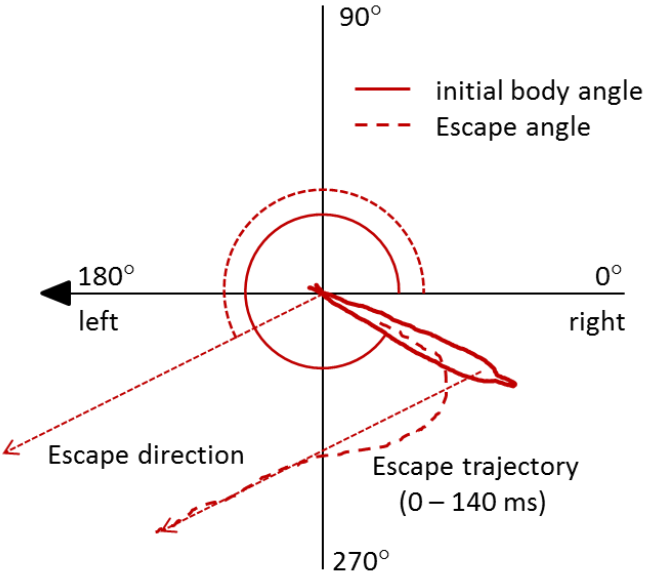

Figure 2.8. The figure illustrates the angles measured for startle responses performed by elephantnose fish in the present study. For clarity, all startle responses performed by initial acceleration to the right were flipped 180° to show all results as if the initial acceleration was from right to left. Thus, *the direction of the initial acceleration* was 180°, indicated by an arrow head in the Figure. *Initial body angle* was the angle of the fish upon startle response with the tail positioned in the origin. Escape direction was determined as the direction of a straight line connecting the initial and the final position of the fish head, and the *escape angle* was the angle of the escape direction. Startle escape *turn angle* was calculated as the absolute value of the angle between initial body angle and escape angle.

imported to a prepared Microsoft Excel 2010 calculation sheet for plotting of startle escape trajectories, and calculations of initial body angle, startle escape angle, total body turn angle, startle escape velocity, startle escape distance and fish length (see Figure 2.8). The initial acceleration direction of the test chamber was varied at random. However, for clarity in figure presentations, escape angles and trajectories are illustrated for the test fish repositioned with the initial head position in the origin, and as if all stimulus accelerations were from right to left. One common stimulus direction was achieved by flipping all trajectories and angles for fish accelerated from left to right by 180°.

Statistical analysis

Comparisons of the different test fish with respect to means of a given response variable were performed by one way ANOVA statistics, while comparisons with respect to median values for non-parametric situations were performed by Kruskal-Wallis statistics. Box plots in the study show median value as line, 70 % percentile as box, 90 % percentiles as bars and outliers as filled symbols. Generalized linear mixed effects candidates models were fitted to examine how startle response probability, startle distance, startle latency and EOD responses in the elephantnose fish depended upon stimulus variables such as level, pressure phase, frequency, and whether they were influenced by fish size and test number. In all candidate models (i.e., different combinations of predictor model structures), fish ID was included as an a priori random effect so as to account for repeated measurements (Zuur et al., 2009). In order to select the candidate model structure that most efficiently balanced prediction precision and bias, the corrected version of Akaike's Information Criterion (Akaike, 1974, Burnham and Anderson, 1998) was used. Comparisons of groups GLMM parameter estimations were conducted in R version 3.2.5 (R Development Core Team, 2016) using package LME4 (Bates et al., 2015). For the remaining tests on model fitting, Stata 13.0 (StataCorp LP, Texas, USA) was used. Figures were prepared using Sigmaplot 13.0 (Systat Software Inc, California, USA). Directionality of startle response trajectories were examined by Rayleigh's R test for uniform (random) directional distribution, Watson-Williams test for equal means, Mardia-Watson-Wheeler tests for equal directional distributions using the software programme Past v2.17c (Hammer et al., 2001).

3 Results

Startle behaviour visualization

Elephantnose fish were gently transferred to the experimental test chamber under dim light conditions, and once in the chamber, they typically swam erratic about exploring the new environment using a high level of EOD-activity. After approximately 3 minutes of set-up preparations, all visible light was turned off, and replaced by the 850 nm IR-laser source for the high speed recording camera and total darkness for the test fish. This caused an immediate change to more relaxed swimming activity, and within 2-3 hours, all test fish were moving calmly around. In addition, they all showed a baseline average EOD-activity. All test fish showed awareness response in the form of transient changes in EOD-activity when

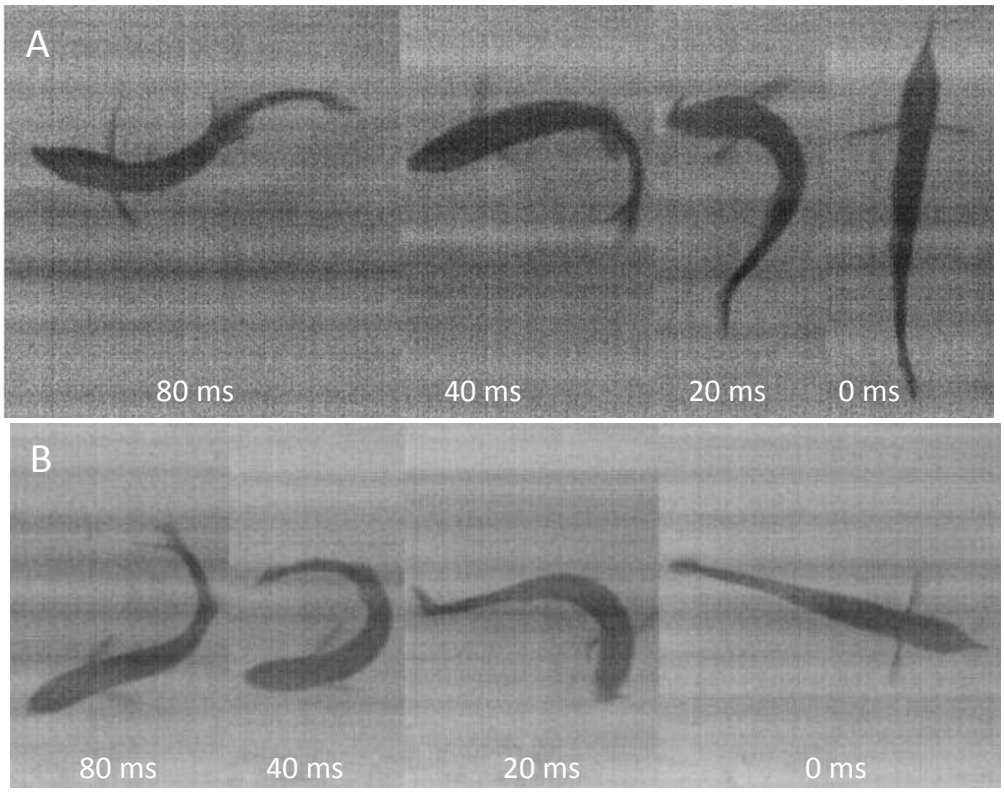

Figure 3.1. High speed (500 fps) and 850 nm IR laser images of elephantnose fish startle behaviours elicited by a 20 Hz initial acceleration towards the left (i.e. 180°). Both fish were in the compression AOI in the test chamber. The four images are from right to left at response onset (0 ms), after 20 ms, after 40 ms and after 80 ms. Fish startle behaviour is characterized by a strong initial C-bend of the body followed by a brief body stretch and forward motion. **(A)** The *initial body angle* of the fish was 90°; it showed an *escape angle* of 180° (i.e. the same as the direction of the initial acceleration), and performed a 90° startle escape *turn angle* to the left. **(B)** The *initial body angle* of the fish was 335°; it showed an *escape angle* of 215°, and performed a 120° *turn angle* to the right. A large turn angle was caused by a stronger and longer lasting initial C-bend phase and by a delayed onset of the body stretch phase.

exposed to the three sound frequencies and levels employed in the study, and at the highest stimulus levels they showed, in addition, clear startle responses. Examples of typical startle behaviour are shown in Figure 3.1. It consisted of a fast and defining initial C-bend of the body followed by a short duration body stretch and forward movement.

Startle response probability

Fish were in a random order exposed to the low frequency acoustic stimuli when inside the compression AOI in the trailing half of test chamber or when inside the rarefaction AOI in the leading half. The levels of initial acceleration and pressure were the same in the two stimulus locations, but pressure phases were opposite. Surprisingly, startle behaviour were, except for one occasion, only triggered when the fish was in the compression AOI. In addition to pressure phase, the probability of startle response depended on both stimulus strength and stimulus frequency (Figure 3.2 A, B). A summary of the number of stimulations and startle responses is given in Appendix 1.

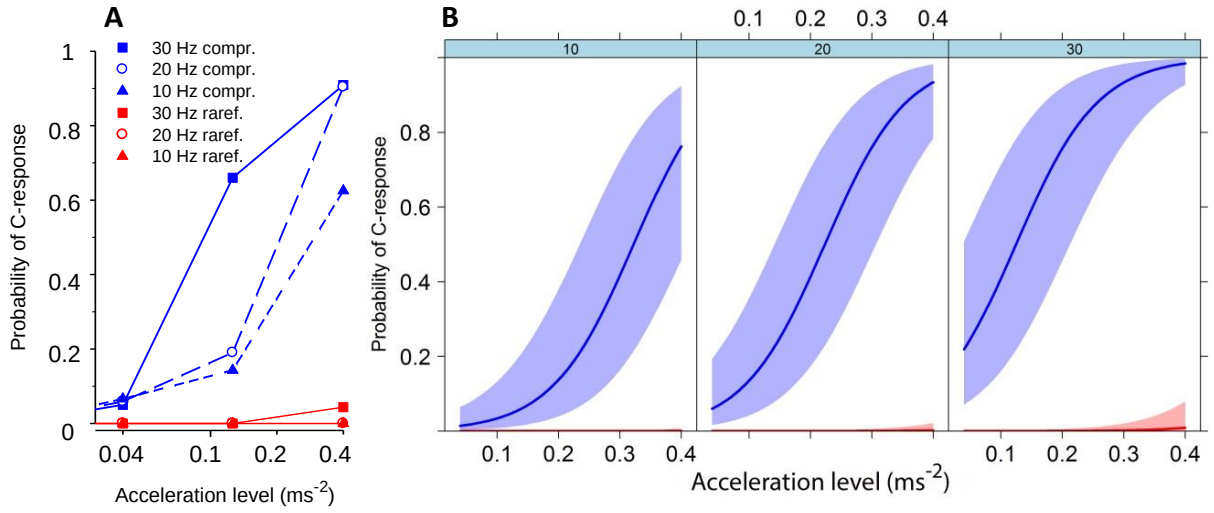

Figure 3.2. (A) Startle response probability in elephantnose fish at three different stimulus levels and frequencies in the compression AOI and rarefaction AOI of the test chamber. Startle behaviour was readily triggered in the compression AOI of the test chamber and only exceptionally in the rarefaction AOI. **(B)** Predicted startle response probabilities and confidence intervals (95 %) based on the best supported logistic mixed effects model of startle response probability (see Table 3.1 and Appendix 1).

Logistic modelling of startle response probability in the compression AOI and the rarefaction AOI as the dependent variable showed best support (Appendix 1) for an additive mixed effects linear model (GLMM) with stimulus strength, stimulus frequency, stimulus phase (Stim phase = 1 equals compression AOI and Stim phase = 0 corresponds to

rarefaction AOI) and fish length as fixed effects explanatory variables (covariates), and with experimental fish treated as a random effect variable (Table 3.1). There was a highly significant and positive effect of stimulus level, compression and of frequency on startle response probability. There was a tendency for a reduced startle response probability in the largest elephantnose fish examined, but this effect was not statistically significant. Predicted startle response probability values with respect to stimulus strength and frequency is shown in Figure 3.2 B.

Table 3.1. *Fixed effects parameter estimates for the most supported logistic GLMM-model (Appendix 1, AICc = 239.9) fitted to predict elephantnose fish startle behaviour probability in the compression AOI versus the rarefaction AOI. Random effects: fish ID.* $R^2c=0.90$ $R^2m=0.84$

Parameter	Estimate	Std. Error	z value	P-value
(Intercept)	-6.7	4.8	-1.4	0.1656
Stim level	15.1	1.7	9.0	2×10^{-16}
Frequency	0.15	0.03	5.3	1.2×10^{-7}
Stim phase	8.8	1.2	7.1	1.0×10^{-12}
Fish length	-0.1	0.1	-1.8	0.0783

Startle response probability in the centre of the test chamber was studied by logistic modelling of startle response probability in the compression AOI and the centre of the test chamber, omitting the data for the rarefaction AOI. The model with best support (Appendix 1) was an additive mixed effects linear model (GLMM) with stimulus strength, stimulus frequency, stimulus position (Stim position = 1 equals compression AOI and Stim position = 0 corresponds to test chamber centre) and fish length as fixed effects variables, and with experimental fish treated as a random effect variable (Table 3.2). There was a highly significant reduced probability for startle behaviour in the centre of test chamber compared to compression AOI in the chamber. Thus initial compression had both an “on-off” effect and a stimulation effect on startle response probability.

Table 3.2. *Fixed effects parameter estimates for the most supported logistic GLMM-model (Appendix 1, AICc = 264.6) fitted to predict elephantnose fish startle behaviour probability in the compression AOI versus the chamber centre. Random effects: fish ID.* $R^2c=0.75$ $R^2m=0.59$

Parameter	Estimate	Std. Error	z value	P-value
(Intercept)	-1.66	4.97	-0.33	0.739
Stim level	15.17	1.71	8.85	2.0×10^{-16}
Frequency	0.16	0.03	5.44	5.2×10^{-8}
Stim position	3.06	0.67	4.54	5.6×10^{-6}
Fish length	-0.09	0.06	-1.60	0.109

Startle response directionality

Initial body angles of elephantnose fish which performed startle behaviour in the compression AOI are illustrated in Figure 3.3, and was not significantly different from that of a random orientation angle distribution (Rayleigh's test, R: 0.1006, P = 0.46). Even though the initial orientations of the fish essentially covered a full circle, startle behaviours by fish in the compression AOI were, irrespective of frequency, strongly directional. In general, they occurred in the direction of the initial acceleration of the test chamber (Figure 3.4 A, B).

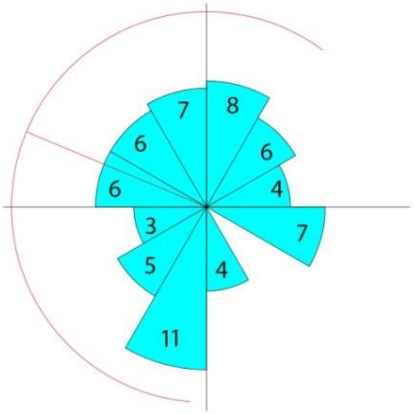

Figure 3.3. Initial body angles of fish performing startle behaviour in the compression AOI. The fish tail is located in the axis centre and each sector is 30°. Numbers within the sector show the number of fish. The scatter of initial body angles was not significantly different from a random angle distribution (Rayleigh's test, R: 0.1006, P = 0.46).

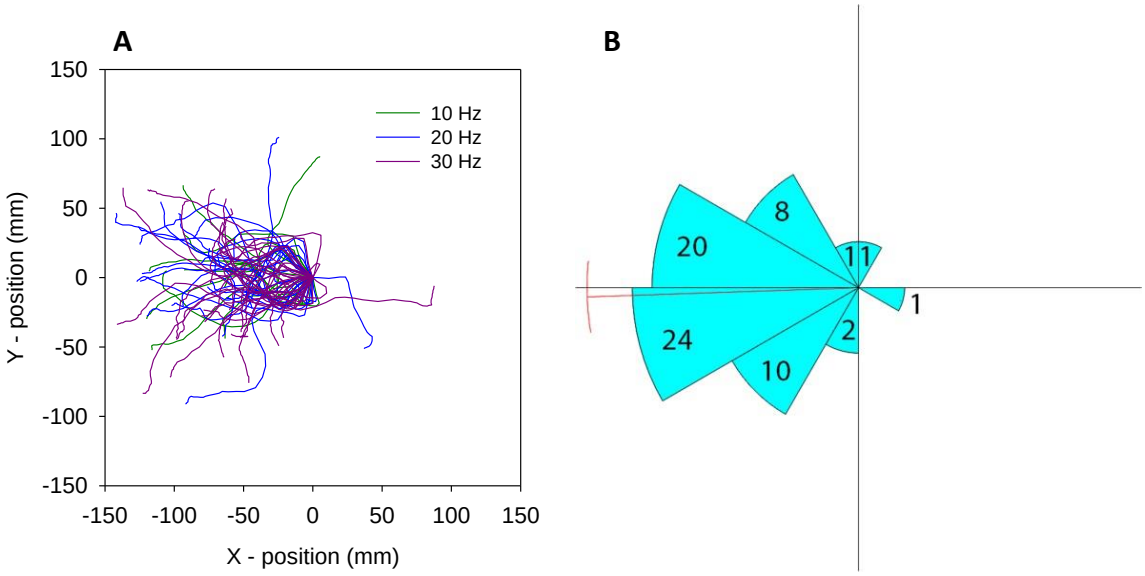

Figure 3.4. (A) Startle response trajectories by elephantnose fish in the compression AOI at 10 Hz – 30 Hz. All C-responses are plotted relative to an initial direction of acceleration of 180°, i.e. stimulation from right to left. **(B)** Sector diagram (sector size 30°) of elephantnose fish escape angles determined from the escape trajectories shown in (A). The mean ± (1 SD) escape angle was 181.9° ± 15.8°, and the distribution was significantly different from that of a uniform distribution (Rayleigh's test, R: 0.8439, P = 4.3 x 10^{-20}).

The combination of the initial orientation of the test fish covering most angles of a full circle, and escape directions being strongly directional, meant that several elephantnose fish in their startle behaviour showed a large body turn angle. This is illustrated in Figure 3.5A which shows startle response trajectories from the compression AOI with all fish reoriented vertically with their initial head position pointing down in the origin. A sector diagram of startle response turn angles, relative to the 270° head down orientation, by fish performing a C-start to the right (probability = $\frac{32}{67}$ = 0.48) and to the left (probability = $\frac{35}{67}$ = 0.52) is shown in Figure 3.5B. The mean ± (1 SD) of the turn angles were 203.1° ± 23.9° for C-turns to the right and 340.4° ± 31.9° for C-turns to the left. Mean turn angles by C-bends to the left and right were not significantly different (Watson-Williams test, P = 0,686), and the left versus right turn angle distributions were not significantly different (Mardia-Watson-Wheeler test, P = 0.172). A sector diagram of all turn angles by fish performing startle behaviour in the compression AOI is shown in Figure 3.5C. The mean ± (1 SD) for this distribution was 68.7° ± 35.1°. Overall, startle responses appeared adaptive in bringing the responding fish away from the flow field of an approaching predator.

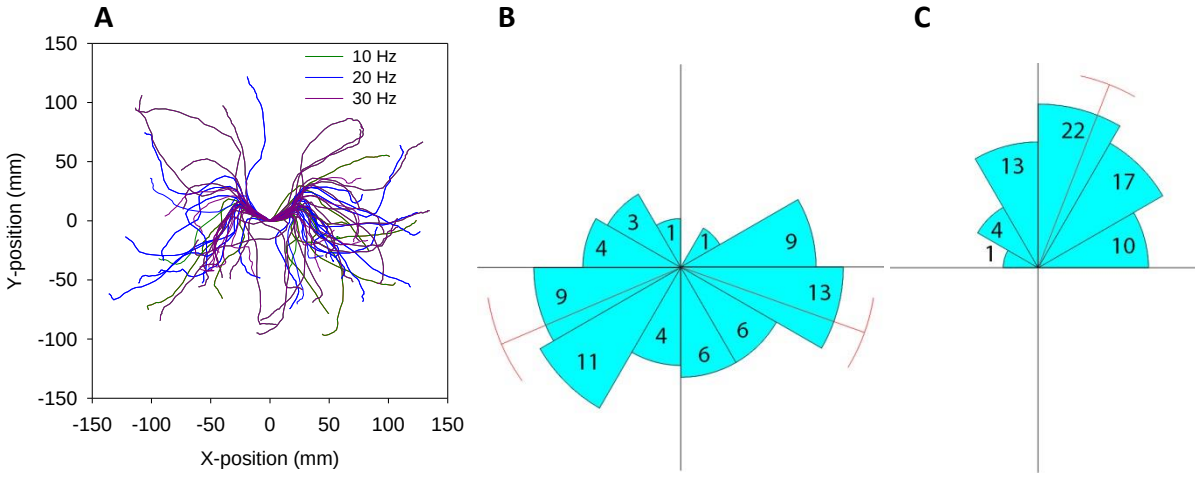

Figure 3.5. (A) Startle response trajectories for startle behaviours in the compression AOI when all elephantnose fish have been reoriented vertically with their head down in the origin, and all stimulations are with initial acceleration from left to right. **(B)** Sector diagram (sector size 30°) of startle response turn angles for the trajectories shown in (A). The left versus right body turn angle were not different with respect to means (Watson-Williams test, P = 0,686) or with respect to distribution (Mardia-Watson-Wheeler test, P = 0.172). **(C)** Sector diagram showing distribution of overall body turn angles by elephantnose fish performing startle behaviour in the compression AOI.

Startle behaviour by fish in the test chamber centre

A total of 9 startle responses were recorded in the tank centre in four different elephantnose fish. The initial body orientation of the fish just prior to startle behaviour is shown in Figure 3.6. Startle response trajectories for the fish responding in the chamber centre is shown in Figure 3.7A. There was a clear tendency for the fish in the centre to escape in the direction of the initial acceleration, but the distribution of startle escape angles

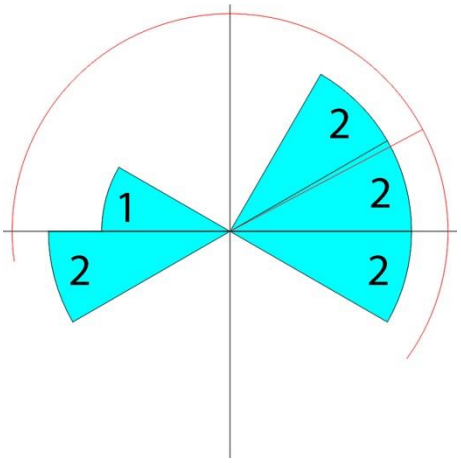

Figure 3.6. Initial body angles of test fish which performed startle behaviour in the chamber centre. The fish tail is located in the axis centre and each sector is 30°. Numbers within the sector show the number of fish. Initial body angles were not significantly different from that of a random angle distribution (Rayleigh's test, R: 0.3909, P = 0.259).

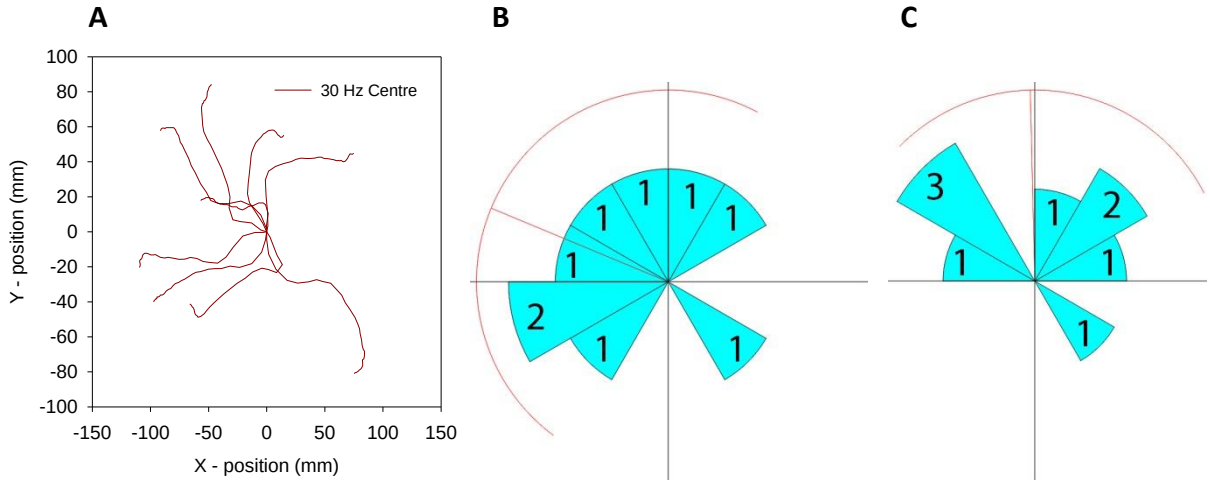

Figure. 3.7. (A) Startle response trajectories by elephantnose fish in the centre of the test chamber at 30 Hz stimulation. All C-responses are plotted relative to an initial acceleration from right to left. **(B)** Sector diagram (sector size 30°) of fish escape angles determined from the escape trajectories shown in (A). The mean ± (1 SD) fish escape angle was 161.6° ± 82.6°, and the distribution was not significantly different from that of a uniform distribution (Rayleigh's test, R: 0.3909, P = 0.259). **(C)** The mean ± (1 SD) of total turn angles were 91.3° ± 85.1°.

(Figure 3.7B) were not significantly different from a uniform distribution (Rayleigh's test, R: 0.3909, P = 0.259). The mean ± (1 SD) total body turn angles by fish performing C-responses in the centre were 91.3° ± 85.1° (Figure 3.7C). The mean and distribution of body turn angles of C-responses in the test chamber centre were not significantly different from those of C-responses in the compression AOI (Watson-Williams test, P = 0.194 and Mardia-Watson-Wheeler test, P = 0.082).

Startle response velocity and distance

Instantaneous speeds of head movements, measured at 4 ms time resolution, during startle behaviours in the compression AOI is shown in Figure 3.8A, B for the frequencies 10 Hz – 30 Hz and the stimulus level 0.4 ms^{-2}. The pattern of head movement and speed was distinct and the same for all observed startle responses. Initially, there was a liner rise in head speed, which peaked at a mean ± (1 SD) of 2.3 ± 0.5 ms^{-1} after 12 ms (Figure 3.8B). This initial transient phase corresponded to the startle response characteristic left or right C-bending of the body. Head movement reached a plateau level of 1.3 – 1.6 ms^{-1} after approximately 20 ms, corresponding to the body stretch and initial forward movement of

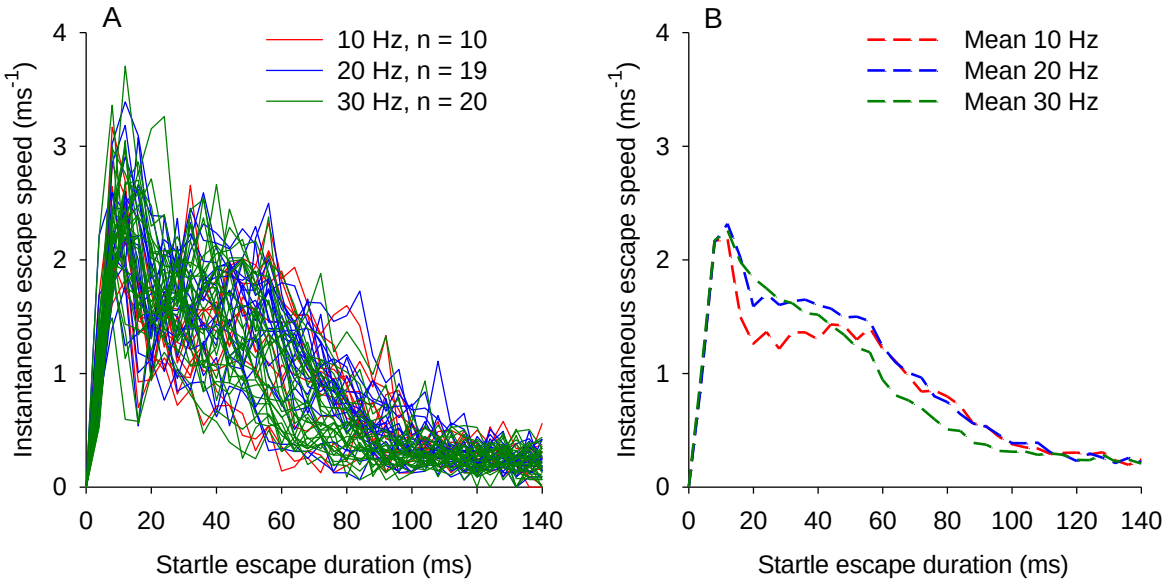

Figure 3.8. (A) Instantaneous speed of head movement, measured at 4 ms time steps, in fish performing startle behaviour in the compression AOI. The stimulus level was 0.4 ms^{-2} for all frequencies. **(B)** Mean escape speeds for the frequencies 10 Hz – 30 Hz, and with standard deviations omitted for clarity. Median values at different time steps were not significantly different (Kruskal-Wallis Test and Dunn's Multiple Comparisons Tests, P > 0.05).

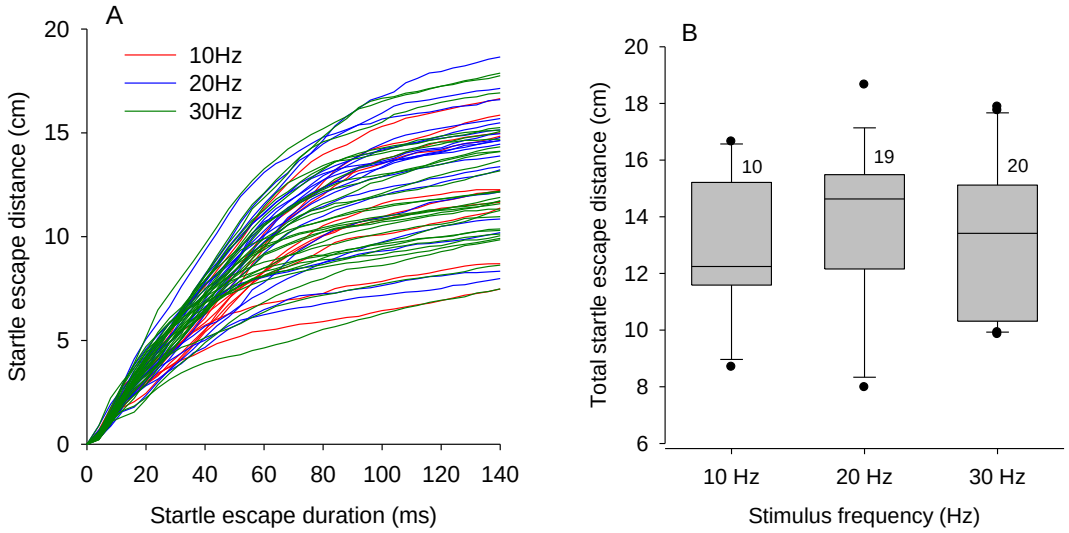

Figure 3.9. (A) Cumulative escape distances measured at 4 ms time steps for startle responses elicited in the compression AOI. The stimulus level was 0.4 ms^{-2} for all test frequencies. **(B)** Box plot of startle escape distance after 140 ms. Means for the different frequencies were not statistically different (One Way ANOVA, F = 1.293, P = 0.283). Numbers indicate sample size.

the fish. The body stretch was followed by a final gliding phase with a decline in the speed of movement back to normal levels within approximately 140 ms. Cumulative startle escape distances for the frequencies 10 Hz – 30 Hz and stimulus level 0.4 ms^{-2}, i.e. comparable to the startle speed calculations, are shown in Figure 3.9A, B.

Typically, the stretch phase of the startle behaviour was accompanied by the fish delivering a single tail stroke before gliding passively until stopping. More occasionally, the body stretch was directly followed by a passive glide, or it was followed by a double tail stroke and then gliding. Thus, the body stretch and gliding phase lasting 80 – 120 ms was a more variable component of the startle behaviour than the initial C-bend. Startle response speeds and distances at the two different stimulus levels 0.13 ms^{-2} and 0.4 ms^{-2} are shown in Figure 3.10A, B. Since there was now significant effect of stimulus frequency, startle response speeds and distances at 10 Hz – 30 Hz were combined. As shown in Figure 3.10A there was no effect of stimulus level on the maximum speed of head movement during the initial C-bending phase. Contrary to this, startle response speed and distance during the body stretch and gliding phase were significantly reduced at the lowest stimulus level (Figure 3.10A, B).

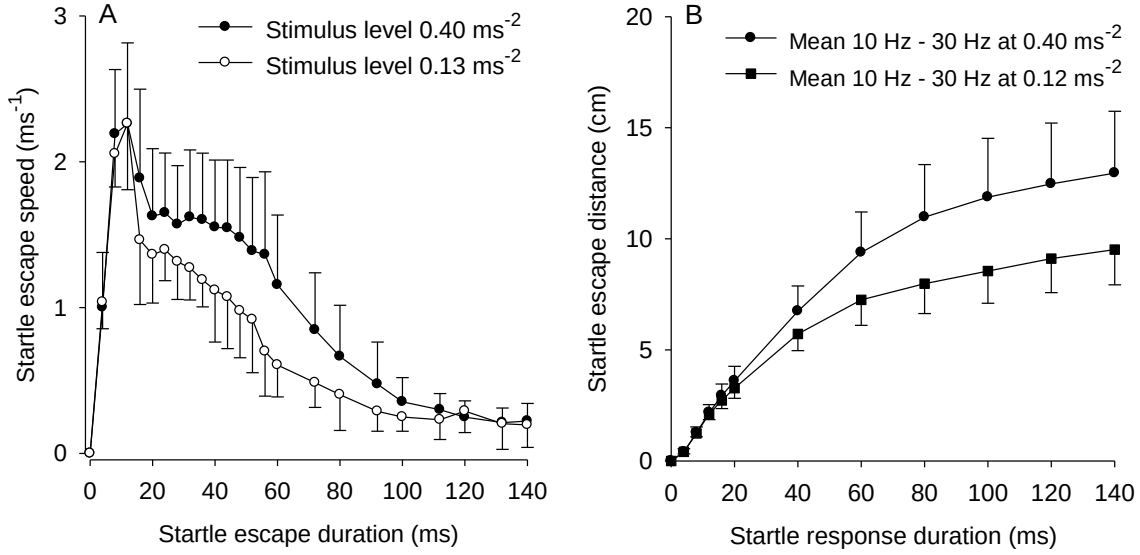

Figure 3.10. (A) Mean speed of head movement (± 1 SD) at different time steps during startle behaviour for 10 Hz – 30 Hz stimulations combined. Maximum head speeds during the transient C-bend of the body was unaffected by the stimulus levels 0.40 ms^{-2} (n = 49 startle responses) and 0.13 ms^{-2} (n = 17 startle responses). Median values of escape speeds in the period 30 ms – 60 ms, i.e. during body stretch and forward movement, were all significantly different (Kruskal-Wallis Test and Dunn's Multiple Comparisons Tests, $P < 0.05$). **(B)** Comparable cumulative escape distances for the two stimulus levels.

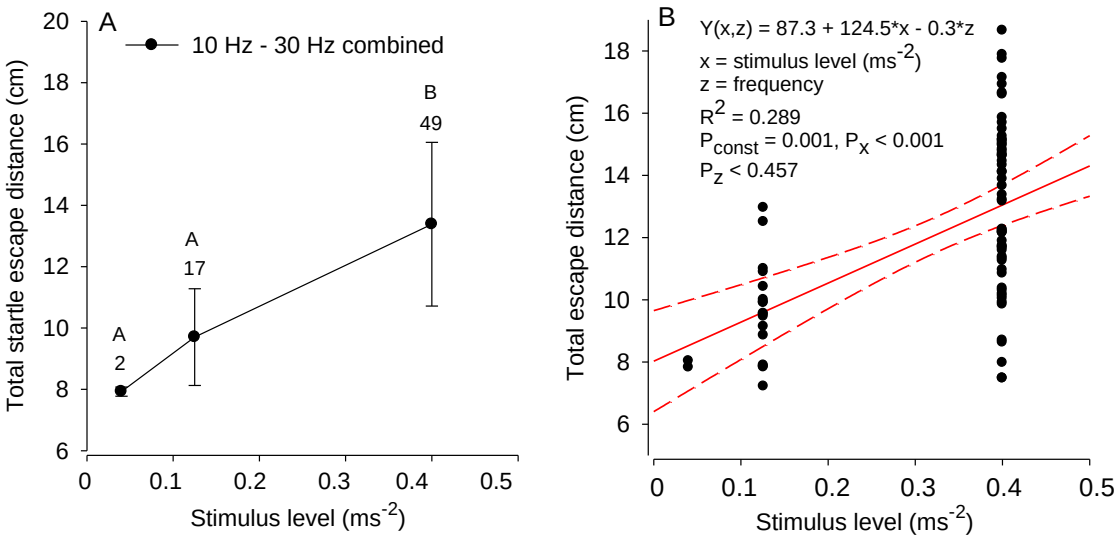

Figure 3.11. (A) Mean startle escape distance after 140 ms (± 1 SD) for the three stimulus levels employed in the study. Startle responses performed at 10 Hz to 30 Hz stimulations were combined. Different letters show groups with significantly different median values (Kruskal-Wallis Test and Dunn's Multiple Comparison's Tests, $P < 0.05$). Number over bar indicates sample size. **(B)** Individual total escape distances in relation to acceleration stimulus level. There was a significant effect of stimulus level but not of stimulus frequency (Multiple linear regression; $P_{constant\ term} < 0.001$, $P_{stimulus\ level} < 0.001$, $P_{frequency} = 0.457$). Regression line and 95 % confidence intervals are shown in red.

Effects of stimulus level on total escape distance, and, thus, on mean escape speeds, are shown in more detail in Figure 3.11A, B. Multiple linear regression analysis confirmed a significant effect of stimulus level on the total escape distance and no significant effect of stimulus frequency (Figure 3.11B). There was, in addition, a significant constant term which is linked to the all or nothing nature of startle behaviour. The constant term of 8.7 cm, i.e. approximately one body length of the experimental fish, is indicative of a stimulus level threshold escape distance. Escape distances fitted a normal distribution (Shapiro Wilk, P = 0.746) but with unequal variance (constant variance test, P = 0.001). A generalised linear mixed effects regression modelling (link identity) of startle escape distance was performed, and showed best support (Appendix 1) for an additive mixed effects model with stimulus level and fish position in the test chamber (i.e. centre = 0 or compression AOI = 1) as fixed effect variables, and experimental fish as the random effects variable. Including frequency and fish length as fixed effects variables in the model, showed that they had no statistically significant effect on total startle escape distance (ANOVA type II Wald F tests, P = 0.9055 and P = 0.8674, respectively). Fixed parameter estimates for the most supported GLMM model is given in Table 3.3.

Table 3.3. *Fixed effects parameter estimates for the most supported additive Gaussian GLMM-model (Appendix 1, AICc = 694.4) fitted to predict total startle distance in the elephantnose fish. Random effects: fish ID.* $R^2c=0.47$ $R^2m=0.34$

Parameter	Estimate	Std. Error	z value	P-value
(Intercept)	54.8	12.3	1.64	0.102
Stim level	143.0	21.7	6.64	9.9×10^{-9}
Fish position	21.1	8.7	-2.41	0.0197

Startle response latency

Startle response latencies of elephantnose fish performing startle behaviour in the compression AOI in the test chamber is shown in Figure 3.12. Groups with significantly different median latency values are indicated in the Figure (Kruskal-Wallis Test and Dunn's Multiple Comparison's Tests, P < 0.05). At the highest stimulus level, with startle response probability close to one, there was a significant difference in startle response latency

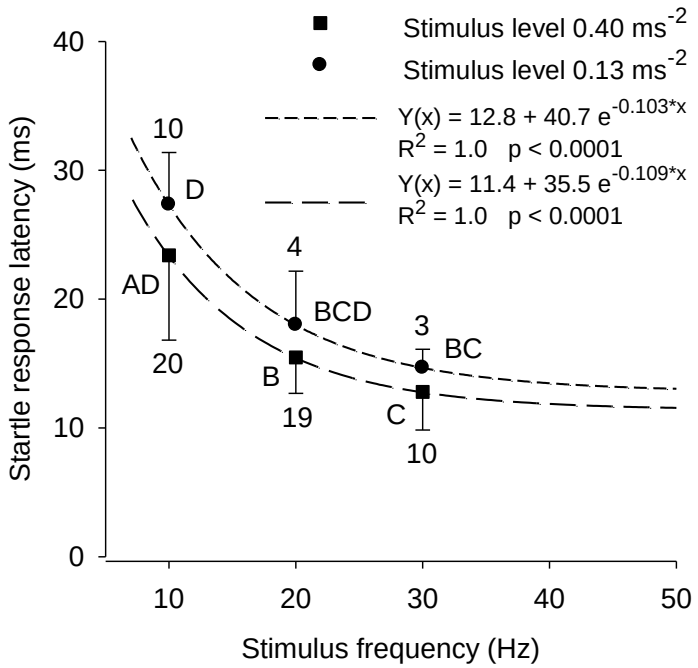

Figure 3.12. Stimulus response latencies (ms) in elephantnose fish which performed startle behaviour in the compression AOI in the test chamber. Startle response latencies were strongly dependent on stimulus level and stimulus frequency. Non-linear regression indicated a latency minimum of approximately 11 ms at high frequency and stimulus levels. Groups with different letters have significantly different median values (Kruskal-Wallis Test and Dunn's Multiple Comparisons Tests, P < 0,05). Number over or under bar indicates sample size.

between all three frequencies examined. At the lower stimulus level (0,13 ms^{-2}), the number of observed startle behaviours was limited. Still, there was a significant difference in latencies between 10 Hz and 30 Hz stimulation. A total of 4 test fish were stimulated at 30 Hz and maximum stimulus level when they were exactly in the chamber centre, i.e. with acceleration associated with no initial pressure changes. A total of 9 startle behaviours were recorded with mean latencies (± 1 SD) of 13.2 ± 2.7 ms. This was not significantly different from the mean latencies (± 1 SD) of 12.8 ± 3.0 ms observed in fish stimulated at 30 Hz and maximum stimulus level in the compression AOI (t-test, t = -0.363, P = 0.719). The number of fish and startle responses examined in the tank centre was low. Still, there appeared to be at most a very limited effect of the position of the fish within the compression half of the test chamber on response latency.

Regression modelling of startle response latency showed best support (Appendix 1) for a mixed effects linear model (GLMM) link Poisson with stimulus level, stimulus frequency, fish length and fish position (i.e. centre = 0 or compression AOI = 1) as fixed effect variables, and experimental fish as the random effects variable. The effect of stimulus level and frequency were highly significant, while the effect of fish length was significant only at the 5 % level. Fish position in the test chamber did not have a significant effect on startle response latency, i.e. contrary to the situation for total escape distance. Fixed effect parameter estimates for the most supported Poisson GLMM-model is given in Table 3.4.

Table 3.4. *Fixed effects parameter estimates for the most supported Poisson GLMM-model (Appendix 1, AICc = 788.6) fitted to predict elephantnose fish startle behaviour latency. Random effects: fish ID.* $R^2c=0.51$ $R^2m=0.48$

Parameter	Estimate	Std. Error	z value	P-value
(Intercept)	3.222	0.292	11.3	$< 2 \times 10^{-16}$
Stim level	-0.825	0.171	-4.84	1.3×10^{-6}
Frequency	-0.031	0.003	-11.2	$< 2 \times 10^{-16}$
Fish length	0.008	0.003	2.5	0.0144
Fish position	-0.138	0.078	-1.8	0.0768

Startle response latency is partly determined by a process of neural integration of acceleration sensitive inner ear nerve activity by the startle response initiating Mauthner cells in the fish brain stem. To examine this aspect, response latencies at maximum stimulations levels were employed to calculate the precise level of acceleration, velocity and displacement of the test fish at the time when startle behaviour was initiated. As indicated in Figure 3.13A, B, C, startle behaviours initiation appeared more related to final stimulus velocity, i.e. the integral of the stimulus acceleration, than to the final level of the acceleration.

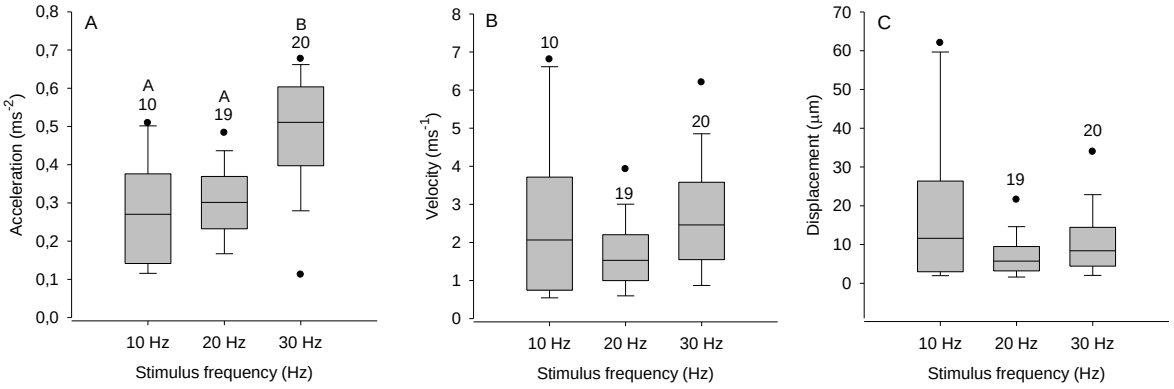

Figure 3.13. (A) Test chamber and test fish level of acceleration, **(B)** velocity and **(C)** displacement at the time of onset of startle behaviour body movement in the compression AOI at 10 Hz – 30 Hz. The stimulus level amplitude of acceleration was 0.4 ms^{-2}. In **(A)** differences in the mean values among the frequency groups which are significant are indicated by letters (One Way ANOVA and Tukey Comparisons Tests, $P < 0.001$). In **(B)** and **(C)** differences in the median velocity and displacement values among the frequency groups are not significantly different (Kruskal-Wallis One Way Analysis of Variance on Ranks, $P_{velocity} = 0.123$ and $P_{displacement} = 0.415$). Number over bar indicates sample size.

Electric organ discharge responses

All elephantnose fish examined emitted very short duration (0.3 ms – 0.4 ms) EODs in a continuous but irregular and occasionally burst-like nature. The amplitude of EODs varies naturally in elephantnose fish and, in addition, it varied slightly with recording distance. Still, EODs could be readily recorded irrespective of the position and movement of the test fish within the test chamber. A typical example of an EOD-recording and an EOD-response during acoustic stimulation and startle behaviour is shown in Figure 3.14. Acoustic stimulations caused a change in the EOD-rate, which generally lasted up to maximum of 2 s. EOD-response was therefore measured as the difference in EOD-count in the 2 s period after and before stimulus onset.

When the test fish had been 2-3 hours in the test chamber in total darkness, they showed a basal level of about 13 to 14 EODs per second measured over 2 s intervals. Pre-stimulus EOD-rates in the 9 elephantnose fish examined is shown in Figure 3.15. The differences in the median values among the different test fish were not significantly different (Kruskal-Wallis test, $P = 0.196$), and the basal level of EOD-rate was therefore sustained throughout the testing.

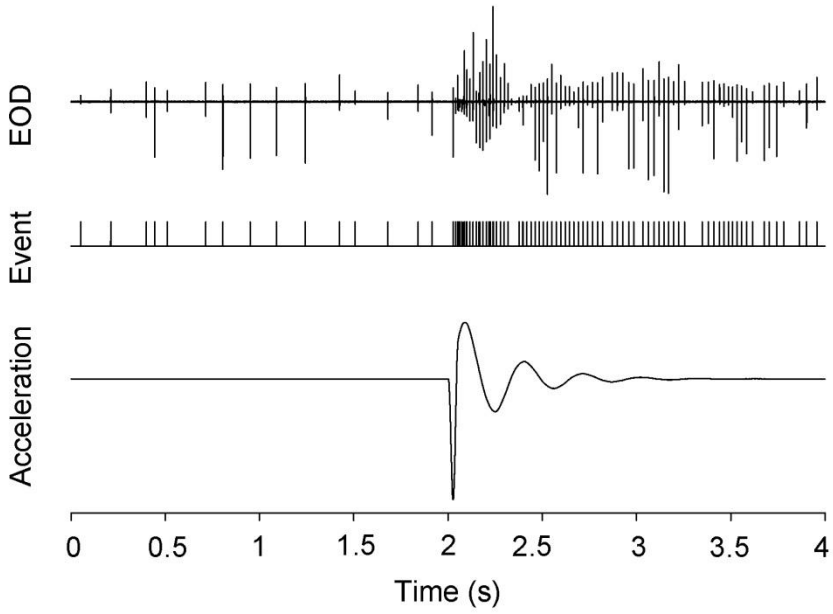

Figure 3.14. The top trace shows an electrophysiological recording of EODs from an elephantnose fish which performed startle behaviour in the compression AOI. The lower trace show the single cycle 20 Hz and 0.4 ms^{-2} stimulus acceleration waveform followed by damped natural oscillations of the test chamber back to the resting position. The stimulus induced increase in EOD-activity began during the 20 Hz stimulus cycle. EODs were detected in the Spike v8.02 recording software, and displayed as 1 V event pulses (centre trace).

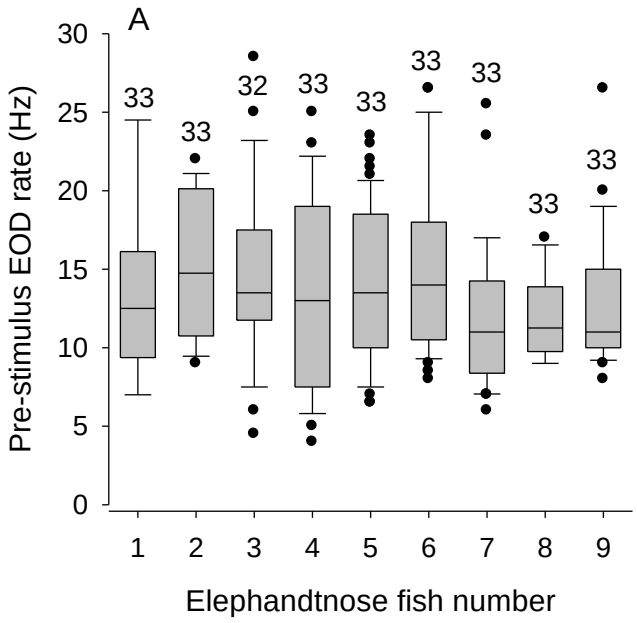

Figure 3.15. Box plot of pre-stimulus EOD-rates in the 9 elephantnose fish examined in the study. Numbers over columns indicate sample size (number of acoustic tests performed). The differences in the median values among the different elephantnose fish examined were not significantly different (Kruskal-Wallis Test and Dunn's Multiple Comparisons Tests, P = 0.196).

A control EOD-response distribution was obtained by randomly selecting 4 s periods of EOD-recordings with no stimulation from the different test fish. In all 50 such periods were obtained and EOD-response to no stimulation measured. A summary of EOD-responses in test fish acoustically stimulated in the compression AOI and the rarefaction AOI respectively, compared to the control is shown in Figure 3.16A, B. There were clear effects of stimulus level and stimulus phase on the EOD-responses, and no apparent effect of stimulus frequency. A change in the EOD-rate to sound pulse stimulation was always positive, i.e. an increase. However, due to the natural irregularity of the EODs, the calculated EOD-response occasionally was a negative value at low stimulus intensities. A non-linear regression of all recorded EOD-responses, i.e. for 10 Hz – 30 Hz stimulations combined, showed that EOD-responses obtained in the compression and rarefaction AOI converged to zero at a stimulus level of 0.0075 ms^{-2} and 0.0092 ms^{-2}, respectively (Figure 3.17A).

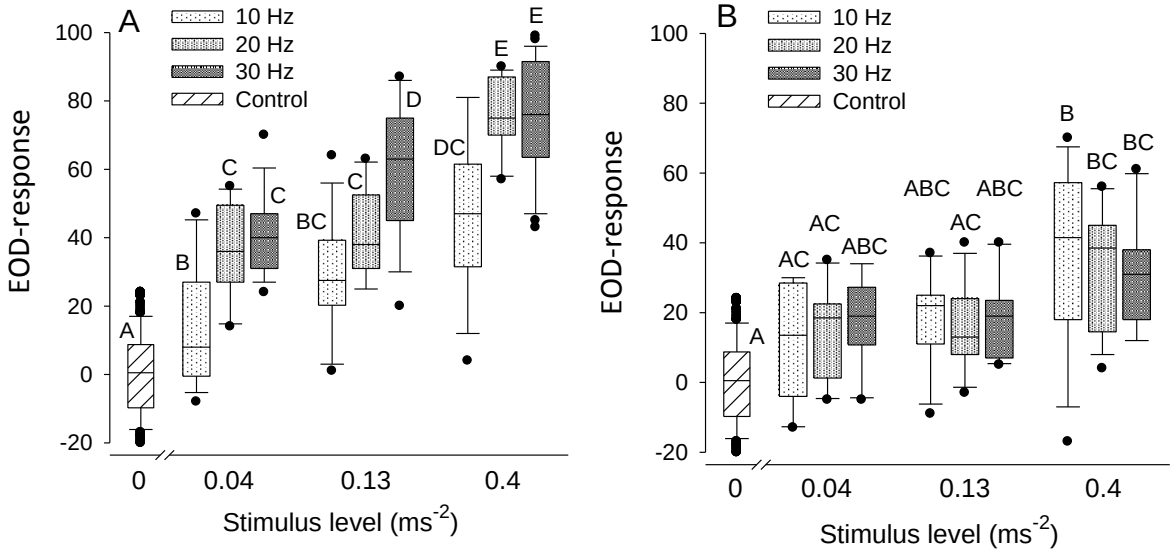

Figure 3.16. (A) Box plots of EOD-responses by elephantnose fish acoustically stimulated in the compression AOI at different stimulus levels and frequencies. **(B)** Box plots of EOD-responses by elephantnose fish stimulated in the rarefaction AOI. The control is EOD-responses to no stimulation. In both figures, different letters indicate groups with significantly different mean values (One Way ANOVA and Tukey Comparison's Tests, $P < 0.05$).

Regression modelling of EOD-responses to the acoustic stimulations showed best support (Appendix 1) for a multilevel mixed effects (GLMM) linear model (link identity) with stimulus level, stimulus frequency, fish length and fish position (rarefaction AOI = value 0, compression AOI = value 1 and centre = value 2) as fixed effect variables, and experimental

fish as the random effects variable. There were statistically significant positive effects of stimulus level and compression AOI. There were no significant effects of frequency, fish length and fish position in the centre (i.e. versus the compression AOI or rarefaction AOI). Fixed effect parameter estimates for the most supported linear GLMM-model is given in Table 3.5. Predicted EOD-responses in the rarefaction and compression AOIs with respect to stimulus level is shown in Figure 3.17B.

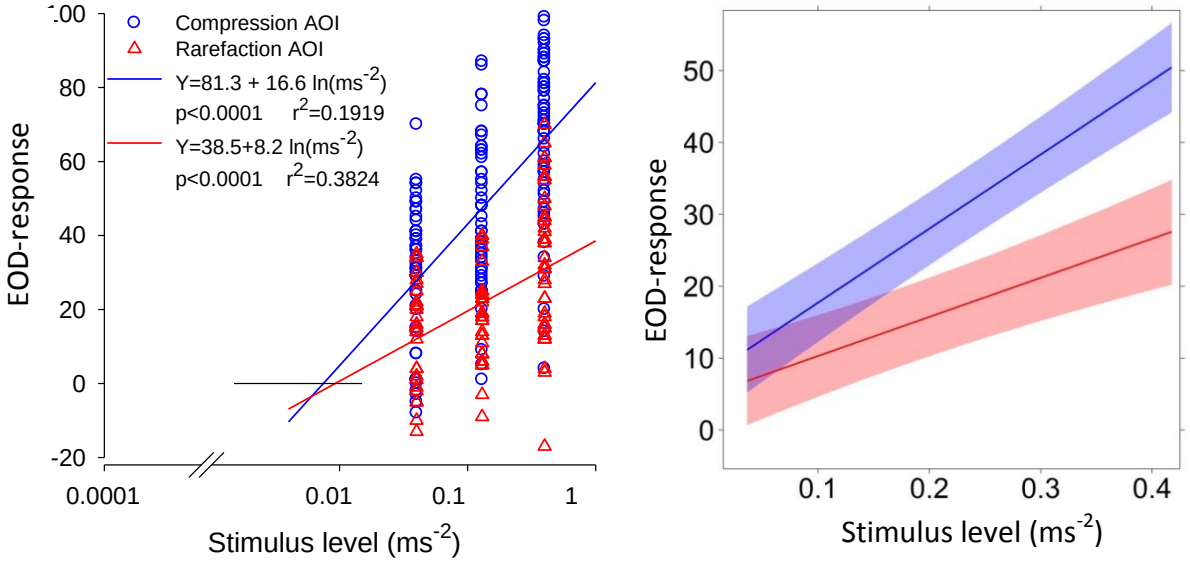

Figure 3.17. (A) Individual EOD-responses by fish stimulated in the compression AOI in the test chamber (in blue) and in the rarefaction AOI (in red) as a function of stimulus level. EOD-responses for each of the employed stimulus frequencies 10 Hz, 20 Hz and 30 Hz were combined. EOD-responses varied considerably due to the natural irregular electric organ discharge in the experimental elephantnose fish. A non-linear regression showed that EOD-responses obtained in the compression and rarefaction AOI converged to zero at a stimulus level of 0.0075 ms^{-2} and 0.0092 ms^{-2}, respectively. **(B)** Predicted EOD-response based on best supported GLMM model (see Table 3.5).

Table 3.5. *Fixed effects parameter estimates for the most supported Gaussian GLMM-model (Appendix 1, AICc = 2509.1) fitted to predict elephantnose fish EOD-response. Random effects: fish ID.* $R^2c=0.71$ $R^2m=0.63$

Parameter	Estimate	Std. Error	z value	P-value
(Intercept)	24.74	15.81	1.56	0.118
Stimulus level	80.95	6.12	13.22	< 0.001
Frequency	0.04	0.12	0.36	0.717
Fish length	-0.13	0.17	-0.75	0.451
Fish position compr	11.93	4.33	2.76	0.006
Fish position centre	-2.32	4.25	-0.55	0.584

4. Discussion

Sensory information eliciting startle behaviour in the test chamber

Elephantnose fish were found to readily respond behaviourally, in a dose-dependent manner, to the low frequency sonic and infrasonic acoustic pulses produced in the test chamber. However, the species has several derived sensory organs, and this makes it important to evaluate the sensory qualities which may be responsible for the startle behaviours and EOD-responses observed.

Elephantnose fish are highly light sensitive through several specialized adaptations (see Lansberger *et al*., 2008), including elongated rods and cones grouped together as "macro-receptor" units into round and light reflecting retinal cups (see introduction for further details). It is well documented that visual stimuli may trigger and influence startle behaviour (see Eaton and Emberley, 1991; Canfield, 2002; Domenici, 2006; Hanke, 2014), and it was therefore important to eliminate any visual cues in the acoustic experiments. Thus, all testing was performed in total darkness except for the 850 nm IR laser to enable video recordings. The IR laser had a very sharp cut off towards shorter wavelength, and was considered outside the visual spectrum of elephantnose fish. This assumption was supported by a lack of change in EODs, which is a typical awareness response in elephantnose fish, when the laser light was turned on and off. It is also supported by observations that elephantnose fish are unable to visually navigate in 880 nm IR led (light-emitting diode) light (Ciali et al., 1997), and the fact that led IR light sources have a poorer short wavelength cut off than IR laser light. In addition, ongoing experiments at the Marine Biological Station in Drøbak have shown that flash light induced startle behaviour in elephantnose fish have significantly longer latencies, due to extra synapses in the afferent pathway to the Mauthner cells, than for the 30 Hz acoustic experiments carried out in this study (Karlsen, personal communication, July, 2016). Thus, visual cues did not trigger or influence the studied startle behaviours. There is still a possibility that the general behaviour in the elephantnose fish was hampered by the total darkness compared to more natural dim light conditions. However, this is not believed to have been the case. Elephantnose fish thrive, feel safe and naturally seek out dark habitats. They are active and behave natural in total darkness, and in such conditions simply switch to rely solely on their acute electric senses and electric organs in gaining information about the surroundings (Schumacher *el al*., 2016). Finally, results from

ongoing experiments at the Marine Biological Station on startle behaviour in elephantnose fish in natural dim light are fully consistent with the findings in total darkness in this thesis (Karlsen, personal communication, July, 2016).

Elephantnose fish have three different types of electrosensory organs named mormyromast organs, knollenorgans and ampullary organs (ampullae of Lorenzini). The ampullary organs are the most electrosensitive of these, and are used by the animals to detection low frequency electric fields produced by other living organisms such as planktonic prey and by predators. The electromagnetic vibrators which drove the test chamber, were powerful and produced electromagnetic fields that potentially could induce electric currents and fields inside the test chamber above thresholds for elephantnose fish ampullary organs. In order to avoid this, all electric cabling to the vibrators were extensively electromagnetically shielded, and each of the vibrators was fitted with a steel Faraday cage. The test chamber, except for the transparent top plate, was also fitted with steel Faraday housing. Possible effects of electromagnetic field were examined by disconnecting the axis between the vibrators and the test chamber, and then passing a maximum level stimulus waveform to the vibrators. This caused the vibrator axis to move, but resulted in no EOD or behavioural response in the elephantnose fish. It was therefore concluded that electromagnetic fields did not affect the startle behaviours. This is also supported by the finding that startle behaviour probabilities were significantly different in the compression AOI, the rarefaction AOI and in the centre of the test chamber, i.e. over small distances within the chamber. This would be very unlikely if the behaviour was driven by electromagnetic fields produced in the experimental room.

Lateral line organs or neuromasts are epidermal mechanosensitive organs which are stimulated by low frequency water flow along the skin of the fish, i.e. by water movement and pressure gradients relative to the skin surface. Since neuromasts have the same density as the surrounding water and the soft body tissues of the fish, they are not stimulated when the fish and water volume are accelerated as a unit (see Bleckmann, 1993; Webb et al., 2007; Bleckmann and Zelick, 2009; Bleckmann and Mogdans, 2014). It is well documented that lateral line stimulation, especially, in the tail and head region, may trigger startle behaviour in fish (Faber and Korn, 1975; Korn and Faber, 1975; Mirjany and Faber, 2011; Mirjany et al., 2011), and as for visual stimuli, stimulation of the lateral line system may modify startle behaviour (Gray, 1984; Canfield and Rose, 1996; Mirjany et al., 2011). In the

present experiments the maximum stimulation level was 0.4 ms^{-2} (amplitude rms), comparable to a maximum pressure of approximately 140 dB re 1 µPa (amplitude rms) at the end walls. The maximum pressure gradient created inside the test chamber was 39.2 Pa/m, which is well above the threshold of 1 Pa/m for lateral line organ stimulation in fish (see Bleckmann and Mogdans, 2014). Still, the lateral line system of the elephantnose fish was not stimulated in the test chamber. The reason is that the swing system was specifically designed to accelerate the experimental fish and the surrounding water together as a unit. Thus, any pressure gradient created will extend through the fish as a whole, and not be relative to body surface. This was confirmed experimentally in an earlier study of startle behaviour in roach (*Rutilus rutilus*) in the test chamber. Specific blocking of the lateral line system in this freshwater species did not affect startle response probabilities and directionality (Karlsen et al., 2004). Boundary layers of poorly defined water movement may occur very close (mm range at most) to the side walls. However, this did not affect the observed startle behaviours, since fish were only stimulated when they were inside an area of interest (AOI), and thereby at least half a body length (4-5 cm) away from the side walls. This distance is, in addition, generally considered to be beyond limits of the distance touch ability of the lateral line system, i.e. the detection of distortions, caused by nearby objects, in the flow field surrounding a swimming fish (see Bleckmann and Zelick, 2009; Bleckmann and Mogdans, 2014). One source of a boundary layer effect in the test chamber is coupled to the pressure gradient developing inside the test chamber initially during stimulation. A water movement inside the chamber, relative to the chamber walls, is necessary to support this pressure gradient. Maximum of such water movement relative to the chamber is produced in the chamber centre, while they will be zero at the end walls. It can be mathematically calculated (not shown in this thesis) that maximum relative water movements in the chamber centre, at a stimulation level of 0.4 ms^{-2}, are in the range of 10^{-7} ms^{-2}. Elephantnose fish have a mechano-, chemo- and electrosensitive nose which is often very close to and also touching the bottom. Theoretically, relative movements and mechanical stress can be created between the tip of the nose touching and following the movement of the chamber and the rest of the fish following the movement of the water inside the chamber. However, this is not considered to have influenced the observed startle behaviours, since 10^{-7} ms^{-2} is well below known thresholds of mechanosensitive skin receptors (free nerve endings and lateral line organs) in fish (see Bleckmann and Mogdans, 2014). In addition, such a

mechanism cannot explain the large difference in startle behaviour probability in the compression AOI compared to the rarefaction AOI.

In conclusion, the acoustic startle behaviours observed in elephantnose fish were most likely elicited by water particle acceleration and pressure acting on the acceleration sensitive inner ear otolith organs and on the pressure sensitive bullae and inner ear saccule system. This means that pressure phase as well as acoustic particle acceleration both had decisive effects on startle response probability and directionality.

Effects of acoustic pressure phase on startle behaviour

A key finding in the present study was that acoustic startle behaviour in elephantnose fish was readily triggered by particle acceleration associated with compression, and very rarely by the same level of particle acceleration associated with rarefaction. In the centre of the chamber, with the same particle acceleration associated with no initial pressure change, startle behaviour was readily triggered but at a significantly lower probability than in the compression AOI in the test chamber. This strongly indicates that an initial pressure decrease (rarefaction) inhibit startle behaviour in elephantnose fish. Results, in addition, showed that particle acceleration alone may trigger startle behaviour, and that initial pressure increase (compression) significantly stimulate and facilitate the response. In fact, it may well be that pressure was as important as particle acceleration in triggering startle behaviour in the compression AOI in the test chamber. A much higher startle response probability caused by an initial compression compared to an initial rarefaction has been documented in the swing chamber set-up in unrelated fish hearing specialist taxa such as cyprinids (Karlsen *et al*., 2004; Eckroth, 2008) and clupeids (Eckroth, 2008; Karlsen and Eckroth, 2011; Hegvik, 2014). Thus, this appears to be a unifying characteristic of fish hearing specialists in general.

In cyprinids separate sensory hair cells and auditory nerves which code acoustic compression and rarefaction have been extensively documented (Furukawa and Ishi, 1967; Furukawa et al., 1972; Piddington, 1972). Similar types of auditory fibres are present in clupeid fish (Enger, 1967), and are most likely present in other systematic groups of fish hearing specialists as well. This suggests that a common trait of fish hearing specialists is for auditory nerves coding particle acceleration and compression to converge on and excite

Mauthner cells as well as additional lower level spinal neurons of the brain stem escape network. Auditory nerves coding rarefaction, on the other hand, may inhibit the escape network. This suggestion that auditory compression and rarefactions fibres in fish hearing specialists connect significantly differently to brain stem Mauthner cells and to brain stem Mauthner cell homologs is new, and may be readily tested in future studies by electrophysiological recordings from Mauthner-cells and/or anatomically by neuronal tracing techniques.

The evolution of acoustic pressure sensitivity in fish

All fish are sensitive to the acoustic vector quantity *sound particle acceleration* by their inner ear otolith organs. In addition, gas-filled bladders in many species play a role in fish hearing by transforming sound pressure variations into mechanical bladder vibrations which can reach and stimulate inner ear otolith organs. Fish hearing specialists are fish which have evolved highly specialized adaptations for an acute such indirect sound pressure sensitivity, and more than 30% of all extant fish species are hearing specialists. In the orders Cypriniformes (carps, minnows and more) and Siluriformes (catfish) auditory adaptations include a chain of small bones, called Weberian ossicles, which effectively transfer sound pressure induced swimbladder pulsations to the saccule otoliths of the inner ears. In Clupeiformes (clupeids) the adaptations include forward swimbladder extensions which end in specialized gas filled bullae located in close proximity to the inner ear utricle otoliths. In Osteoglossiformes (elephantnose fish and others) the specializations include two small and separate gas-filled vesicles closely associated with the inner ear saccule otolith. Clearly, adaptations for pressure sensitivity in fish hearing specialists are highly diverse, and have evolved independently several times (see Ladich and Popper, 2004; Braun and Grande, 2008; Popper and Ketten, 2008; Ladich, 2010; 2014).

Striking predator fish produce mainly low frequency (<50 Hz) frontal bow waves of particle accelerations associated with an initial pressure increase. In the wake of the attacking fish, however, a flow field of particle accelerations associated with pressure decrease is produced. Since predator evasive startle behaviours in all systematic groups of fish hearings specialists studied so far are mainly triggered by particle acceleration and compression, it is highly likely that the acute inner ear pressure sensitivity in fish hearing

specialists have evolved as adaptations to detect close distance (near field) low frequency compressions in order to evade attacks by striking predators. In this context, it makes sense that the fish should not perform startle behaviour, and thereby reveal its presence, when it experiences a strong initial rarefaction signal.

Fish are highly vocal, and produce sounds by specialized sonic muscles attached to the swimbladder, by grinding of body structures and more (see Popper et al., 2003; Ladich, 2010; 2014). Many fish groups such as cod fish are known to produce species specific sounds of great importance during mate selection, courtship and spawning. An alternative mechanism for the evolution high level pressure sensitivity in fish could therefore have been to improve sound communication (see Braun and Grande, 2008; Ladich, 2014). However, this hypothesis does not fit the fact that barely any species within the order Cypriniformes have been found to produce sound. In addition, most sound producing fish are not hearing specialists.

Swimbladders in fish hearing specialists have resonance frequencies close to 1 kHz, and their upper auditory frequency limit is typically a few kHz. This is far higher than the 200 – 600 Hz upper frequency cut off in fish hearing non-specialists. Thus, adaptations for increased pressure sensitivity may have evolved to extend the auditory range. However, this seems unlikely since biologically produced sounds are mainly of low frequency, well below 100 Hz (Bleckman et al., 1991). In fact, the biological importance of hearing in the kHz range in fish hearing specialists is still in many cases unclear.

Startle behaviour thresholds

Startle response thresholds in the elephantnose fish in the compression AOI were approximately 0.2 ms^{-2} – 0.05 ms^{-2} (amplitude rms) in the frequency range 10 Hz – 30 Hz, corresponding to acoustic pressures in the AOIs of about 148 – 134 dB re 1 µPa. In the same experimental set-up as employed in the present study, startle response threshold at 6.7 Hz was approximately 0.03 m/s^2 in the fish hearing specialist roach (Karlsen et al., 2004) and approximately 0.01 m/s^2 at 20 Hz in the fish hearing specialist sprat (Hegvik, 2014). Thus, startle response thresholds in the elephantnose fish were in the order of 12-18 dB higher than in roach and sprat. In the compression AOI in the test chamber, startle responses in roach, sprat and elephantnose fish were all triggered by a combination of acceleration and

pressure stimulation of the inner ear. Thus, the elevated thresholds in elephantnose fish may indicate that low frequency inner ear pressure sensitivity is less developed in this species compared to the carp and clupeid fish species. Hegvik (2014), in addition, determined startle response thresholds in acoustic pressure insensitive young salmon to be in 0.1 m/s^2 at 20 Hz. This was close to 20 Hz acceleration startle thresholds in the elephantnose fish.

No other studies have examined low frequency startle thresholds in fish. At higher frequencies, Casagrand et al. (1999) found the acceleration thresholds for detection of excitatory postsynaptic potentials (EPSPs) from M-cells in the carp species goldfish to be around 0.01 m/s^2 at 125 Hz. Casagrand et al. (1999) also recalculated the sound pressure threshold given by Lewis and Rogers (1996), for eliciting directional startle behaviours in goldfish, to an acceleration threshold of 0.03 m/s^2. Blaxter et al. (1981) and Blaxter and Hoss (1981) found the particle acceleration threshold for acoustic startle in the clupeid species herring to be within the range 0.01–0.04 m/s^2 in the frequency range 70 Hz – 200 Hz. These more high frequency thresholds are very close to the infrasonic and very low frequency sonic thresholds found in the swing chamber set-up.

Startle responses directionality

Startle behaviours triggered in elephantnose fish in the compression AOI in the test chamber were highly directional. Overall, they occurred in the direction of the initial acceleration, irrespective of the initial orientation of the fish. In terms of predator-prey interactions, escapes would be away from a charging predator and thereby increase survival. Pressure is a scalar quantity, and the directionality of the startle behaviours must therefore be due to detection of the particle acceleration component of the acoustic stimulus by the directional and particle acceleration sensitive inner ear otolith organs. Moreover, stimulus directionality was extracted by the fish within a few milliseconds, and it was, thus, clearly a time domain (i.e. integration with respect to time) and not a frequency domain analysis.

The leading current model for directional hearing in fish is the so called phase model (Shuijf, 1975; 1981; Buwalda et al., 1983). In short, the model states that a fish in a sound field cannot tell the direction to a sound source based on detection of acoustic particle acceleration alone because there will always be a 180° ambiguity. This ambiguity in the

particle motion can, according to the model, only be resolved if the fish is able to separately detect pressure phase. The reason is that sound induced particle motion towards a sound source (monopole) is associated with a pressure increase, while particle motion away from the source is associated with a pressure decrease. Thus, by comparing particle acceleration and pressure phase, the fish will be able to resolve the 180° ambiguity, and decide the direction to at least a simple monopole sound source. The phase theory mainly focuses on analyses of pressure phase and particle accelerations over several periods of a sound stimulus, i.e. analyses in the frequency domain. Contrary to this, startle behaviour directionality was found to be a very fast time domain process. Most likely, the initial particle acceleration detected by the otolith organs is directly transferred to the Mauthner cells and the neural escape network to give an appropriate directional response. Since the behaviour takes place in the near field with an increased ratio of particle accelerations to pressure compared to the far field, directionality based directly on the initial particle acceleration would appear to be a natural mechanism. Acoustic pressure and pressure phase are clearly important in startle behaviour, but rather than being an input to a neural mechanism of phase-particle motion comparison (i.e. as stated in the phase model), pressure appears to directly facilitate (initial compression) or inhibit (initial rarefaction) the Mauthner cells and the behaviour. Still, the precise nervous coupling of different inner ear auditory fibre types and the super-fast brain stem escape network neurons is still unknown.

Based on the phase model, it has been proposed that acoustic pressure sensitivity evolved in fish hearing specialists as a means for directional hearing and sound source localization (see Braun and Grande, 2008; Popper and Ketten, 2008; Ladich, 2014). However, this view is not supported by the results of this study, since directionality of the startle responses in the elephantnose fish most likely were directly related to detection of the direction of the initial imposed acceleration of the fish. This conclusion is supported by studies of startle responses in small (5 cm - 7 cm) salmon in the same set-up as employed for the elephantnose fish study. The young salmon were insensitive to sound pressure, but still showed highly directional startle responses in the same overall direction as the initial acceleration of the test chamber (Hegvik, 2014). Morover, startle response probabilities were the same in the compression AOI and the rarefaction AOI in the salmon. Thus, the acoustic pressure sensitivity in fish hearing specialists assists in deciding when a startle response is appropriate (during compression and attack by a striking predator).

Startle response velocity and distance

Startle behaviour is generally considered to be a fixed all or nothing reflex type of behaviour consisting of a stereotypic initial C-bend followed by a body stretch phase of varying directionality (see Faber et al., 1989; 1991; Korn and Faber, 1996; Zottoli and Faber, 2000; Eaton et al., 2001). Typically, the response has duration of about 140 ms, and total startle distance, i.e. the movement of the fish head, typically covers 1-2 body lengths (see Eaton et al., 2001). However, startle distance in relation to stimulus strength has not been examined in detail previously. In the present study, total startle distance was found to be significantly affected by stimulus level. It ranged from approximately 1 body length at startle response threshold levels to 1.3 – 1.9 body lengths at the stimulus level when startle response probability was close to 1. This is the first time such a relation has been documented, and it strongly indicates that increased activation of the inner ear leads to stronger and more extensive activation of the brain stem escape network. In addition, there was a significant effect of position of the fish in the centre of the chamber versus the compression AOI. This effect was small, and it was coupled to the fish in the centre making overall larger body turn angles before the body stretch than in the compression AOI. Startle response speed and distance during the initial C-bend of the body was not affected by stimulus strength, and this is consistent with the all or nothing view of startle behaviour. Contrary to this, the following body stretch and gliding phase were graded responses highly dependent on stimulus strength. Modulation and variability of the startle response is, thus, coupled to the second phase of the behaviour, and thereby to activation of brain stem spinal neurons other than the Mauthner cell. Fish length and stimulus frequency had little variation in the study, and did thus not affect startle response distance.

The speed of the head movement during the initial C-bend of the body was observed to increase steadily to an average maximum value of 2.3 ms^{-1} after 12 ms. This corresponds to an impressive average acceleration of 191.7 ms^{-2} or 19.5 g during the initial stage of the C-response. There are few comparable studies, but the values for elephantnose fish correspond well with the observed maximum head speed of 2.2 ms^{-1} after 15 ms of startle behaviour in a 7.3 cm angelfish (*Pterophyllum eimekei*) (Domenici and Blake, 1991). Following the initial C-bend, a maximum average whole body speed of 1.6 ms^{-1} was observed within 20 ms – 40 ms in the elephantnose fish. This corresponds to a maximum body velocity

to body length ratio (V_{max}/L ratio) of approximately 1.6 (ms^{-1}) / 0.08 (m) = 20.0. This is well within the ratio range of 1 – 100, which has been documented in animals ranging from bacteria to African bush elephants and whales (Meyer-Vernet and Rospars, 2015). For fish in particular, a regression of maximum (sprint) swimming speed (ms^{-1}) against body length (m) is reported by Domenici (2001) in the form log V_{max} = 0.49 log L + 0.60. Entering the length (L) of the elephantnose fish studied, this regression equation returns a predicted V_{max} of 6.3 ms^{-1} in this species. This is 394% higher than the maximum forward body speed observed during the startle response in the elephantnose fish. It is not surprising that maximum body speed following a single body C-bend and stretch (i.e. the startle response) is lower than the maximum speed following several high frequency and high power swimming strokes (i.e. a swimming sprint). Maximum swimming sprint responses (called S-responses) are occasionally triggered in test fish in the experimental set-up employed in the study instead of C-bend startle behaviours. The total escape distance within 140 ms of S-responses are always significantly lower than for a C-type startle response (Karlsen, personal communication, July, 2016). Thus the C-type startle behaviour is a better predator evasive movement with respect to speed and distance within a short time interval than an S-response. A swimming sprint, even though it results in a higher swimming speed over time, has a lower survival value than an abrupt jump to the side (C-startle).

Acoustic startle response latencies

Mean startle response latencies in elephantnose fish in the compression AOI at a stimulus level of 0.4 ms^{-2} (amplitude rms) were 12.7 ms at 30 Hz, 15.4 ms at 20 Hz and 23.7 ms at 30Hz. There was significant effects of stimulus frequency, stimulus level and fish length on the response latency. The fish length correlation coefficient was positive showing that larger fish had larger stimulus latencies, and this may be linked to an increase in length of nerve pathways and thereby conduction time with body size. In an earlier study in the same experimental set-up (Hegvik, 2014), mean startle response latencies in 5-7 cm long sprat was 30.6 ms at a stimulus level of 0.1 ms^{-2} at 20 Hz. This is nearly twice the latency found in the elephantnose fish at a 12 dB higher stimulus level. The observed higher startle response thresholds in elephantnose fish compared to sprat is, thus, in terms of startle escape effectiveness, compensated for by shorter response latency.

At the level of sensory organs and neurons of the brainstem escape network, the response latency has two main components. The first component includes activation of the inner ear otolith organs and integration of direct auditory nerve input by the startle response initiating Mauthner cells. This component is expectedly variable, and as shown for elephantnose fish, dependent on stimulus level as well as stimulus rise time (i.e. frequency). The second component of the stimulus latency is the time from one of the Mauthner cells reaches threshold and fires it's single action potential until body movement can be observed. This second phase is expectedly fixed in duration as it involves non-variable processes such as Mauthner cell nerve conduction, synaptic transmissions and muscle cell activation. At the highest stimulus level of 0.4 ms^{-2}, startle response latency asymptotically approached a value of 11.4 ms as frequency increased. Compared to maximum observed startle response latencies of 35 ms, the variable component of the startle latency in the elephantnose fish was 3 – 4 times the fixed duration component. Biologically, this reflects a large capacity for neural integration in the Mauthner cells, and a broad frequency tuning of the startle behaviour.

Fish otolith organs behave as nearly critically damped accelerometers, in which sensory hair cell stimulation at low frequencies (< 100 Hz) is proportional to the level of stimulus acceleration (i.e. test chamber acceleration in the employed set-up). Auditory nerve input to the Mauthner cells should therefore reflect the stimulus acceleration. By integrating stimulus acceleration, the activation of the M-cells and startle response latencies should be linked to the stimulus velocity more than stimulus acceleration. This was indeed found to the case.

EOD-responses to the acoustic stimulations

Weakly electric fish like the elephantnose fish navigate and explore their dark and turbid environment by active electrolocation and electrocommunication. This involves the generation of EODs, and detailed mapping of the fields surrounding the fish by specialized electrosensitive organs. In the present study, an average EOD-rate of about 14 Hz was reached when the test fish had been 2-3 hours in total darkness in the test chamber. During testing, differences in pre-stimulus EOD-rates did not vary significantly between the different elephantnose fish examined or throughout the testing period. The pre-stimulus EOD-rate of

about 14 Hz is above the EOD-rate of 3 – 8 Hz previously described for elephantnose fish at rest (Moller, 1995; von der Emde, 1998). This indicates, as would be expected, that the fish were slightly agitated and not fully in a resting status when acoustically tested in the experimental set-up.

A key finding in the study was that EOD-responses differed significantly in magnitude in the compression and the rarefaction AOI in the test chamber, just as the situation for startle response probability. The response was positively correlated the stimulus level, and unaffected by frequency, fish length and whether the fish was stimulated in the centre or the compression AOI in the test chamber. This fits with the observed EOD-responses being orienting or “novelty responses” (Meyer, 1982; von der Emde, 1999). Surprisingly however, the EOD-response was reduced by initial rarefaction. One argument for such a mechanism could, as for startle response probability, be that reduced EOD-response reduces the chance for the fish revealing its presence in the wake of a potential predator. Given that the combined acceleration and compression stimulus was interpreted as a predatory attack by the elephantnose fish, one could argue that a natural response should be EOD-inhibition, i.e. in order not to further reveal its presence. On the contrary, it could be that a burst of EODs is both informative to elephantnose fish, and potentially may function as an evasion aiding distraction or noise signal towards predatory fish such as Siluriformes and others which use their own highly developed electric senses during feeding. A strong EOD-response associated with startle behaviour in elephantnose fish can perhaps be compared to a squid combining ink release and a jet-escape in order to confuse and distract as well evade the predator.

It is well established that weakly electric fish can respond to changes in their environment with a "novelty response" consisting of change in the rate of their EODs (Meyer, 1982; von der Emde, 1999; Caputi et al., 2003; Engelmann et al., 2009). Depending on stimulus level, EOD-rates have been shown to increase up to 100 Hz in elephantnose fish (von der Emde, 1999; Engelmann et al., 2009). How EOD-rate is measured and defined varies in different studies. A conservative approach of counting EODs over a 2 s period following stimulus onset was chosen in the present study. Even though EOD-rate declined during the 2 s interval, EOD-response rates of 40 – 50 Hz were readily recorded during stimulation in the compression AOI at the highest stimulus level. The change in EOD-rate to the acoustic stimuli eliciting startle behaviours was therefore substantial. Stimulus onset versus EOD-response latencies were not studied in detail. However, the change in EOD-rate to the

acoustic stimuli clearly occurred very fast and within 50 - 100 ms. Thus, it was certain that the EOD-responses observed were driven by the initial phase of the acoustic stimulus. Following the driving voltage waveform and the designed acoustic stimulus, the test chamber showed a damped 4-5 Hz oscillation back to its resting position. This damped oscillation was significantly lower in amplitude than the initial acoustic stimulus, and is not considered to have significantly affected the measured EOD-responses.

Hearing range and sound production in elephantnose fish

Weakly electric fish within the family Mormyridae, including the elephantnose fish, are highly vocal and produce sounds for both territorial defence and courtship. Typically, the sounds are tone bursts with fundamental frequencies in the range 300 Hz to 500 Hz, referred to as moans, grunts, hoots, clicks and growls (Rigley and Marshall, 1973, Crawford et al., 1997a; 1997b; Fletcher and Crawford, 2001). The sound pressure levels of the sounds produced are typically about 130 dB re 1 µPa measured at a distance of 10 cm, and clearly mormyrid fish must have an auditory capacity to allow for their acoustic communications. McCormick and Popper (1984) studied behavioural pure tone hearing thresholds in elephantnose fish from 100 Hz to 2500 Hz. They documented an upper frequency limit of 2-3 kHz, and found best sensitivity frequencies in the range 300 Hz to 1000 Hz with thresholds of about 70 dB re 1 µPa. The upper frequency range and best frequency thresholds are comparable to what has been found in other groups of fish hearing specialists (see review by Ladich and Schulz-Mirbach, 2016). In a follow up study, Fletcher and Crawford (2001) studied pure tone hearing thresholds in elephantnose fish in the same frequency range of 100 Hz to 2500 Hz, but measured EOD-responses rather than performance of a learned behaviour response. The audiogram they obtained using the EOD-response, was virtually identical to the behavioural audiogram. This strongly indicates that elephantnose fish show EOD-response to acoustical stimuli at levels down to hearing threshold. In the present study it was found that EOD-responses converged to zero at stimulus levels of 0.0075 ms^{-2} (compression AOI) and 0.0092 ms^{-2} (rarefaction AOI). An auditory stimulus is typically detected only when it is approximately 20 dB above any masking background noise (see Popper et al., 2003; 2008). Thus, the results indicate either an auditory threshold of 7.5 10^{-3} ms^{-2} (corresponding to a pressure of about 122 dB re 1 µPa in the compression AOI), or a

masking background noise level of approximately 7.5 10^{-4} ms^{-2} was present in the test chamber, or that EOD-responses are not shown down to threshold levels at very low frequencies. Further studies are needed to clarify these questions in detail.

In the present study, the hearing range of elephantnose fish has been documented down to 10 Hz, i.e. well into the infrasound range. This in fact constitutes an extension of the auditory range in this species by more than 3 octaves, and is therefore nearly comparable to the previously established 4-5 octaves of hearing above 100 Hz. Fletcher and Crawford (2001) showed that auditory thresholds at 100 Hz and above were due to sound pressure detection via the gas-filled bubble coupled to the sacculus in each inner ear. In the present study the inner ear acoustic pressure sensitivity has been extended to 10 Hz and the infrasonic range. Moreover, it has been shown that elephantnose fish are able to detect and behave differentially to pressure phase at such low frequencies. This raises the question of why the acute acoustic pressure sensitivity has evolved in elephantnose fish and other fish hearing specialists. Is it to allow for high frequency sound communications, or to detect very low frequency sound pressures in order to better avoid predatory attacks? Recently, this has been referred to as “one of the riddles of sensory physiology” (Ladich and Schulz-Mirbach, 2016). As argued above, the results of this study favours the predator-prey hypothesis.

5 Conclusions

Acoustic startle behaviours in the elephantnose fish hearing specialist were found to be elicited in the compression AOI of approximately 0.2 – 0.05 m/s^2 (amplitude rms) in the frequency range 10 Hz – 30 Hz, respectively, i.e. by a stimulus mimicking key components in the acoustic signatures of a charging predator attack. Directionality of the startle behaviours was provided by acoustic particle acceleration, i.e. the kinetic sound component. The primary aims of this master thesis were summarized into four hypotheses. This shows the concrete answers to these four hypotheses, based on the results and experiments done in this master thesis.

H01: The hearing range of the weakly electric species elephantnose fish was found to extend below 100 Hz because the acoustic stimuli in the frequency range 10 Hz to 30 Hz triggered both C- and EOD-responses. The null-hypothesis prediction must therefore be rejected.

H02: Acoustic startle behaviour in elephantnose fish was found to be elicited by both acoustic particle acceleration and acoustic pressure. Particle acceleration provided directionality to the startle behaviours, while acoustic compression stimulated the response. Acoustic rarefaction was found to inhibit startle behaviour. The null-hypothesis must therefore be rejected.

H03: EOD-rate was found to be affected by the low frequency (10 Hz, 20 Hz and 30 Hz) acoustic stimuli. Acoustic compression had a stronger effect on EOD-rate than rarefaction. The threshold value for EOD-response was about 10^{-3} ms^{-2}. The null-hypothesis must therefore be rejected.

H04: Startle behaviours triggered in the frequency range 10 Hz to 30 Hz were strongly influenced by pressure phase. Initial compression stimulated the behaviour, while initial rarefaction inhibited startle responses. The null-hypothesis prediction must therefore be rejected.

6 References

Akaike, H. (1974). A new look at the statistical model identification. IEEE Transac. Automa. Contr. 19:716-723.

Bates, D., Maechler M., Bolker B. and Walker S. (2015). Fitting Linear Mixed-Effects Models using lme4. Journ. Stat. Soft.: http://arxiv.org/abs/1406.5823.

Blaxter, J. H. S. and Hoss, D. E. (1981). Startle response in herring: the effect of sound stimulus frequency, size of fish and selective interference with the acoustico-lateralis system. J. Mar. Biol. Ass. U.K. 61:871-897.

Blaxter, J. H. S., Denton, E. J. and Gray, J. A. B. (1981). The auditory bullae-swimbladder system in late stage herring larvae. J. Mar. Biol. Ass. U.K. 61:315-326.

Bleckmann, H. (1993). The role of lateral line in fish behaviour. In: Behaviour of teleost fishes, ed. Pitcher, T. J., pp. 201-246. New York: Springer Verlag.

Bleckmann, H. and Mogdans, J. (2014). Neuronal basis of source localisation and processing of bulk water flow with the fish lateral line. In: Flow Sensing in Air and Water, eds. Bleckman, H., Mogdans, J. and Coombs, S. L., pp. 371-398. New York: Springer Verlag.

Bleckmann, H. and Zelick, R. (2009). Lateral line system of fish. Integr. Zool. 4:13-25.

Bleckman, H., Breithaupt, T., Blickhan, R. and Tautz, J. (1991). The time course and frequency content of hydrodynamic events caused by moving fish, frogs and crustaceans. J. Comp. Physiol. 168:749-757.

Braun, C. B. and Grande, T. (2008). Evolution of Pheripheral Mechanisms for the Enhancement of Sound Reception. In: Fish Bioacoustics, eds. Webb, J. J., Fay, R. R. and Popper, A. N., pp. 99-144. New-York: Springer Verlag.

Burnham, K. P., and Anderson, D. R. (1998). Model Selection and Inferences. New-York: Springer Verlag.

Buwalda, R. J. A., Schuijf, A. and Hawkins, A. D. (1983). Discrimination by cod of sounds from 0pposing directions. J. Comp. Physiol. 150:175-184.

Canfield, J. G. (2002). Functional evidence for visuospatial coding in the Mauthner neuron. Brain. Behav. Evol. 67:188-202.

Canfield, J. G. and Rose, J. G. (1996). Hierarchial sensory guidance of Mauthner-mediated escape responses in Goldfish (*Carassius auratus*) and chichlids (*Haplochromis burtoni*). Brain Behav. Evol. 48:137-156.

Caputi, A. A., Aguilera, P. A. and Castelló, M. E. (2003). Probability and amplitude of novelty responses as a function of the change in contrast of the reafferent image in *G. carapo*. J. Exp. Biol. 206: 999-1010.

Casagrand, J. L., Guzik, A. L. and Eaton, R. C. (1999). Mauthner and reticulospinal responses to the onset of acoustic pressure and acceleration stimuli. J. Neurophysiol. 82:1422-1437.

Ciali, S., Gordon, J. and Moller, P. (1997). Spectral sensitivity of the weakly disharching electric fish *Gnathonemus petersii* using its electric organ dischargeing response measure. J. Fish Biol. 50: 1074 – 1087.

Crawford, J. D. (1997). Hearing and acoustic communication in mormyrid fishes. Mar. Fresh. Physiol. 29:65-86.

Crawford, D. J., Cook, A. P. and Heberlein, A. S. (1997a). Bioacustic behaviour of African fishes (Mormyridae): potential cues for species and individual recognition in Pollimyrus. J. Acoust. Soc. Am. 102: 1200-1212.

Crawford, D. J., Jacob, P. and Bénech. V. (1997b). Sound production and reproductive ecology of strongly acoustic fish in Africa: *Pollimyrus isidori*, Mormyridae. Behav. 134:677-725.

Domenici, P. (2001). The scaling of locomotor performance in predator-prey encounters: from fish to killer whales. Comp. Biochem. Physiol. A. 131: 169-182.

Domenici, P. (2006). The visuallay mediated escape response in fish: predicting prey responsiveness and the locomotor behaviour of predators and prey. Mar. Fresh. Behav. Physiol. 35:87-110.

Domenici, P. and Blake, R. W. (1991). The kinematics and performance of escape response in the angelfish (*Pterophyllium eimekei*). J. Exp. Biol. 156: 187-205.

Eaton, R. C. and Emberley, D.S. (1991). How stimulus direction determines the trajectory of the Mauthner-initiated escape response in a teleost fish. J. Exp. Biol. 161:469-487.

Eaton, R. C. and Popper, A. N. (1995). The octavolateralis system and Mauthner cell: interactions and questions. Brain Behav. Evol. 46:124-130.

Eaton, R. C., Canfield, J. C. and Guzik, A. L. (1995). Left-right discrimination of sound onset by the Mauthner system. Brain Behav. Evol. 46:165-179.

Eaton, R. C., Lee, R. K. K. and Foreman, M. B. (2001). The Mauthner cell and other identified neurons of the brainstem escape network of fish. Prog. Neurobiol. 63:467-485.

Eckroth, J. (2008). Directionality and adequate stimulus of acoustic startle responses in fish hearing specialists and generalists. Master thesis University of Oslo.

Engelmann, J., Nöbel, S., Röver, T. and von der Emde, G. (2009). The Scnauzenorgan-response of *Gnathonemus petersii*. Front. Zool. 21: 1-15. Doi:10.1186/1742-994-6-21.

Enger, P. S. (1967). Hearing in herring. Comp. Biochem. Physiol. 22:527-538.

Faber, D. S. and Korn, H. (1975). Inputs from the posterior lateral line nerves upon the goldfish Mauthner cell. Evidence that the inhibitory components are mediated by interneurons of the recurrent collateral network. Brain Res. 96:249-356.

Faber, D. S., Fetcho, J. R. and Korn, H. (1989). Neural networks underlying the escape response in goldfish. Ann. NY Acad. Sci. 563:11-33.

Faber D. S., Korn H. and Lin J. W. (1991). Role of medullary networks and postsynaptic membrane properties in regulating Mauthner cell responsiveness to sensory excitation. Brain Behav. Evol. 37:286-297.

Fine, M. L. and Parmentier, E. (2015). Mechanism of fish sound production. In: Sound communication in fishes, ed. Ladich F., pp.78-126. Wien: Springer-Verlag.

Fishlore (2016) *Elephantnose Fish*, [online], available: http://www.fishlore.com/aquariummagazine/june09/elephantnose-fish.htm [accessed 20 July 2016].

Fletcher, J. B. and Crawford, J. D. (2001). Acoustic detection by sound-producing fishes (Mormyridae): the role of gas-filled tympanic bladders. J. Exp. Biol. 204: 175-183.

Furukawa, T. and Ishi, Y. (1967). Neurophysiological studies on hearing in goldfish. J. Neurophysiol. 30:1377-1403.

Furukawa, T., Ishii, Y. and Matsuura, S. (1972). Synaptic delay and time course of postsynaptic potentials at the junction between hair cells and eighth nerve fibers in the goldfish. Jap. J. Physiol. 22:617-635.

Gray, J. A. B. (1984). Interaction of sound pressure and particle acceleration in the excitation of the latral-line neuromasts of sprat. Proc. R. Soc. Lond. B 220:299-325.

Hammer, Ø., Harper, D. A. T. and Ryan, P.D. (2001). PAST: Paleontological statistics software package for education and data analysis. Palaeont. Electron. 4:1-9. http://palaeo-electronica.org/2001_1/past/issue1_01.htm.

Hanke, W. (2014). Natural hydrodynamic stimuli. In: Flow Sensing in Air and Water, eds. Bleckman, H., Mogdans, J. and Coombs, S. L., pp. 3-29. New York: Springer Verlag.

Hegvik, S. (2014). Acoustic startle responses in European sprat (*Sprattus sprattus L.)* and diploid versus triploid Atlantic salmon fry (*Salmo salar L.).* Master thesis University of Oslo.

Hopkins, C. D. (1986). Behavior of Mormyridae. In: Electroreception, ed. Bullock, T. H. and Heiligenberg, W. F., pp. 527-576. New York: John Wiley and Sons.

Kalmijn, A. J. (1989). Functional evolution of lateral line and inner ear sensory systems. In: The mechanosensory lateral line, eds. Coombs, C., Görner, P. and Münz, H., pp. 187-216. Amsterdam: Elsevier.

Karlsen, H. E. (1992a). The inner ear is responsible for detection of infrasound in the perch (*Perca fluviatilis*). J. Exp. Biol. 171:163-172.

Karlsen, H. E. (1992b). Infrasound Sensitivity in the Plaice (*Pleuronectes platessa*). J. Exp. Biol. 171:173-187.

Karlsen, H. E. and Eckroth, J. R. (2011). Terskelverdier for lydpulsindusert startle-atferd hos ulike arter og hørselsgrupper av fisk, og effekter av lydpulser på spisemotivasjon. Report to the Norwegian Petroleum Directorate. 43 pp.

Karlsen, H. E., Piddington, R. W., Enger, P. S. and Sand, O. (2004). Infrasound initiates directional fast-start escape in juvenile roach *Rutilus rutilus*. J. Exp. Biol. 207:4185-4193.

Korn, H. and Faber, D. S. (1975). Inputs from the posterior lateral line nerves upon the goldfish Mauthner cell. Properties and synaptic localization of the excitatory component. Brain Res. 96:342-348.

Korn, H. and Faber, D. S. (1996). Escape - brainstem and spinal cord circuitry and function. Curr. Opin. Neurobiol. 6:862-832.

Kreysing, M., Pusch, R., Haverkate, D., Landsberger, M., Engelmann, J., Ruiter, J., Mora-Ferrer, C., Ulbricht, E., Grosche, J., Franze, K., Streif, S., Schumacher, S., Makarov, F., Kacza, J., Guck, J., Wolburg, H., Bowmaker, J. K., von der Emde, G., Schuster, S., Wagner, H. J., Reichenbach, A. and Francke, M. (2014). Photonic crystal light collectors in fish retina improve vision in turbid water. Science 338: 1700-1703.

Ladich, F. (2010). Hearing: Vertebrates. In: Encyclopedia of Animal Behaviour, ed. Ladich, F., pp. 54-60. Vienna: Elsevier.

Ladich, F. (2014). Fish bioacoustics. Curr. Opin. Neurobiol. 28:121-127.

Ladich, F. and Popper, A. N. (2004). Parallel evolution in fish hearing organs. In: Evolution of the Vertebrate Auditory System, eds. Manley, G. A., Popper, A. N. and Fay, R. R., pp. 95-127. New York: Springer Verlag.

Ladich, F. and Schulz-Mirbach, T. (2016). Diversity in fish auditory systems: one of the riddles of sensory biology. Ecol. Evol. 28 doi . 10.3389/fevo.2016.00028.

Landsberger, M., von der Emde, G., Haverkate, D., Schuster, S., Gentsch, J., Ulbricht, E., Reichenbach, A., Makarov, F. and Wagner, H. J. (2008). Dim light vision – morphological and functional adaptations of the eye of the mormyrid fish, *Gnathonemus petersii*. J. Physiology Paris 102: 291-303.

Lewis, T. N. and Rogers, P. H. (1996). The vibrational response of single-chambered fish swimbladders to low-frequency sound. ICES J. Mar. Sci. 53: 285–287.

Liu, H., Huang, Y. and Jiang, H. (2016). Artificial eye for scoptic vision with bioinspired all-optical photosensitivity enhancer. Proc. Natl. Acad. Sci. 113:3982-3985.

McCormick, C. A. and Popper, A. N. (1984). Auditory sensitivity and physiological tuning curves in the elephantnose fish, *Gnathonemus petersii*. J. Comp. Physiol. A 155:753-761.

Meyer, J.H. (1982). Behavioral responses of weakly electric fish to complex impedances. J. Comp. Physiol. 145:459-470.

Meyer-Vernet, N. and Rospars, J. P. (2015). How fast do living organisms move: maximum speeds from bacteria to elephants and whales. Am. J. Phys. 83:719-722.

Mirjany, M. and Faber, D. S. (2011). Characteristics of the anterior lateral line nerve input to the Mauthner cell. J. Exp. Biol. 214:3368-3377.

Mirjany, M., Preuss, T. and Faber, D. S. (2011). Role of the lateral line mechanosensory system in directionality of goldfish auditory evoked response. J. Exp. Biol. 214:3358-3367.

Moller, P. (1995). *Electric fishes. History and Behaviour*. London: Chapman and Hall.

Piddington, R. W. (1972). Auditory discrimination between compressions and rarefactions by goldfish. J. Exp. Biol. 56:403-419.

Popper, A. N. and Ketten, D. R. (2008). Underwater hearing. In: The Senses: A Comprehensive Reference, eds. Basbaum, A. I., Kaneko, A., Shepherd, G. M., Westheimer, G., Albright, T. D., Masland, T., Dallos, P. and Oertel, D., pp. 225-236. Vienna: Elsevier.

Popper, A. N., Fay, R. R., Platt, C. and Sand, O. (2003). Sound detection mechanisms and capabilities of teleost fishes. In: Sensory Processing in Aquatic Environments, eds. Collen, S. P. and Marshall, N. J., pp. 3-38. New York: Springer Verlag.

R Development Core Team. (2016). R: a language and environment for statistical computing. 3.2.5 edition. R Foundation for Statistical Computing (http://www.R-project.org.), Vienna, Austria.

Rigley, L. and Marshall, J. (1973). Sound production by the elephant nose fish, *Gnathonemus petersii* (Pisces, Mormyridae). *Copeia* 19: 134–135.

Sand, O. and Karlsen, H.E. (1986). Detection of infrasound by Atlantic cod. J. Exp. Biol. 125:197-204.

Sand, O. and Karlsen, H. E. (2000). Detection of infrasound and linear acceleration in fishes. Philos. Trans. R. Soc. London 355:1295-1298.

Schuijf, A. (1975). Directional hearing of cod under approximate free field conditions. J. Comp. Physiol. 98:307-332.

Schuijf, A. (1981). Models of acoustic localization. In: Hearing and Sound Communication in Fishes, eds. Tavolga, W. N., Popper, A. N. and Fay, R. R., pp. 267-310. New York: Springer Verlag.

Schumacher, S., de Perera, T. B., Thenert, J. and von der Emde, G. (2016). Cross-modal object recognition and dynamic weighting of sensory inputs in a fish. Proc. Natl. Acad. Sci. 113:7638-7643.

Von der Emde, G. (1998). Capacitance detection in the wave-type electric fish Eigenmannia during active electrolocation. J. Comp. Physiol. A. 182: 217-224.

Webb, J. F., Montgomery, J. C. and Mogdans, J. (2007). Bioacoustics and the lateral line system of Fishes. In: Fish Bioacoustics, eds. Fay, R. R., Webb, J. F. and Popper, A. N., pp. 145-182. New York: Springer Verlag.

Zottoli, S. J. and Faber, D. S. (2000). The Mauthner cell: what has it taught us? Neuroscientist 1:26-38.

Zuur, A., Ieno, E.N., Walker, N., Saveliev, A.A., Smith, G.M. (2009). Mixed Effects Models and Extensions in Ecology with R. New York: Springer Verlag.

7 Appendix

Appendix 1

Ranked generalized linear model (GLM and GLMM) selection tables based on AICc-values. K: numbers of parameters estimated, AICc: the corrected (according to number of observations) Akaike's Information Criterion, Delta AICc: the difference in AICc value of the particular model and the most supported model. The most supported models (with a delta AICc-value less than two) are shown in bold.

Logistic GLM and GLMM model selection of **elephantnose fish startle response probability in the compression AOI versus the rarefaction AOI**.

GLM model structures	**K**	**AICc**	**∆AICc**
Stim level + stim phase + fish length +frequency	5	265.3	0.0
Stim level * stim phase + fish length + frequency	5	267.1	1.8
Stim level * stim phase * frequency + fish length	5	268.9	3.6
Stim level * stim phase * frequency	4	285.1	19.8
Stim level + stim phase + fish length	4	289.9	24.6
Stim level + stim phase	3	306.2	40.9
Stim level * stim phase	3	307.9	42.6
GLMM model structures	**K**	**AICc**	**∆ AICc**
Stim level + stim phase + fish length + frequency + (1 I fish ID)	6	239.9	0.0
Stim level + stim phase + frequency + (1 I fish ID)	5	240.6	0.7
Stim level + stim phase * frequency + (1 I fish ID)	6	241.0	1.1
Stim level * stim phase + fish length + frequency + (1 I fish ID)	7	241.8	1.9
Stim level * stim phase + frequency + (1 I fish ID)	6	242.5	2.6
Stim level + stim phase + (1 I fish ID)	4	277.6	37.7

Logistic GLM and GLMM model selection of **elephantnose fish startle response probability in the compression AOI versus the test chamber centre**.

GLM model structures	**K**	**AICc**	**∆AICc**
Stim level + stim position + fish length +frequency	5	285.2	0.0
Stim level * stim position + fish length + frequency	5	286.5	0.3
Stim level * stim position * frequency + fish length	5	286.8	0.7
Stim level * stim position * frequency	4	300.3	18.1
Stim level + stim position + fish length	4	318.5	33.3
GLMM model structures	**K**	**AICc**	**∆ AICc**
Stim level + stim position + frequency + fish length + (1 I fish ID)	6	264.6	0.0
Stim level + stim position + frequency + (1 I fish ID)	5	265.1	0.5
Stim level * stim position + fish length + frequency + (1 I fish ID)	6	266.5	1.8
Stim level * stim position + frequency + (1 I fish ID)	7	268.0	2.3
Stim level + stim position + frequency + (1 I fish ID)	6	307.0	42.3

Gaussian GLM and GLMM model selection of **elephantnose fish startle escape distance in the compression AOI versus the test chamber centre**.

GLM model structures	**K**	**AICc**	**Δ AICc**
Stim level +fish position + fish length + frequency	5	1403.4	0.0
Stim level + fish position	3	1404.9	1.5
Stim level	2	1410.8	7.4
Stim level * fish position*frequency + fish position	5	1411.9	8.5
GLMM model structures	**K**	**AICc**	**Δ AICc**
Stim level + fish position + (1 I fish ID)	5	694.4	0.0
Stim level + (1 I fish ID)	4	698.0	3.6
Stim level + fish position + fish length + frequency + (1 I fish ID)	7	699.1	4.7
Stim level + fish length + (1 I fish ID)	5	700.0	5.6
Stim level + frequency + (1 I fish ID)	5	700.0	5.6
Stim level + fish length + frequency + (1 I fish ID)	6	702.1	7.7
Stim level * fish position + (1 I fish ID)	5	704.4	10.0

Poisson GLM and GLMM model selection of **elephantnose fish startle response latency in the compression AOI versus the rarefaction AOI**.

GLM model structures	**K**	**AICc**	**Δ AICc**
Stim level +fish position + fish length + frequency	5	1403.4	0.0
Stim level + fish position	3	1404.9	1.5
Stim level	2	1410.8	7.4
Stim level * fish position*frequency + fish position	5	1411.9	8.5
GLMM model structures	**K**	**AICc**	**Δ AICc**
Stim level + frequency + fish length + fish position (1 I fish ID)	6	788.6	0.0
Stim level + frequency + fish length + (1 I fish ID)	5	789.5	0.9
Stim level + frequency + (1 I fish ID)	4	791.1	2.5
Stim level + (1 I fish ID)	3	903.7	115.1
Stim level + fish position (1 I fish ID)	4	904.6	116.0

Gaussian GLM and GLMM model selection of **elephantnose fish EOD-response in the compression AOI versus the rarefaction AOI**.

GLM model structures	**K**	**AICc**	**Δ AICc**
Stim level + stim position	4	5020.3	0.0
Stim level * stim position + fish length	5	5020.5	0.2
Stim level * stim position + fish length + frequency	5	5022.4	2.1
Stim level * stim position	3	5039.6	19.3
GLMM model structures	**K**	**AICc**	**Δ AICc**
Stim level + frequency + fish length + stim position + (1 I fish ID)	6	2509.1	0.0
Stim level + stim position + fish length + (1 I fish ID)	7	2510.6	1.5
Stim level * stim position + fish length + frequency + (1 I fish ID)	8	2512.7	3.6

Stim level * stim position * fish length + (1 I fish ID)	10	2516.7	7.6
Stim level * stim position * fish length + frequency + (1 I fish ID)	11	2518.8	9.7
Stim level * stim position + (1 I fish ID)	5	2519.4	10.3
Stim level + stim position + fish length + (1 I fish ID)	6	2520.9	11.9
Stim level * stim position + fish length + frequency +(1 I fish ID)	7	2523.0	13.9

Appendix 2

Number of acoustic tests and number of C-responses observed in the elephantnose fish.

Frequency and position	Acceleration ms^{-2}	Pressure dB re 1µ Pa	Number of tests	Number of C-responses
10 Hz compr AOI	0.4	149	16	10
10 Hz compr AOI	0.13	139	14	2
10 Hz compr AOI	0.04	129	15	1
10 Hz rarefr AOI	0.4	- 149	18	0
10Hz rarefr AOI	0.13	- 139	16	0
10 Hz rarefr AOI	0.04	- 129	9	0
20 Hz compr AOI	0.4	149	21	19
20 Hz compr AOI	0.13	139	16	3
20 Hz compr AOI	0.04	129	17	1
20 Hz rarefr AOI	0.4	- 149	18	1
20 Hz rarefr AOI	0.13	- 139	18	0
20 Hz rarefr AOI	0.04	- 129	9	0
30 Hz compr AOI	0.4	149	22	20
30 Hz compr AOI	0.13	139	18	12
30 Hz compr AOI	0.04	129	14	0
30 Hz rarefr AOI	0.4	- 149	17	0
30 Hz rarefr AOI	0.13	- 139	16	0
30 Hz rarefr AOI	0.04	- 129	9	0
30 Hz centre	0.4	0	13	9

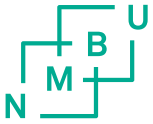

Norges miljø- og biovitenskapelig universitet
Noregs miljø- og biovitskapelege universitet
Norwegian University of Life Sciences

Postboks 5003
NO-1432 Ås
Norway